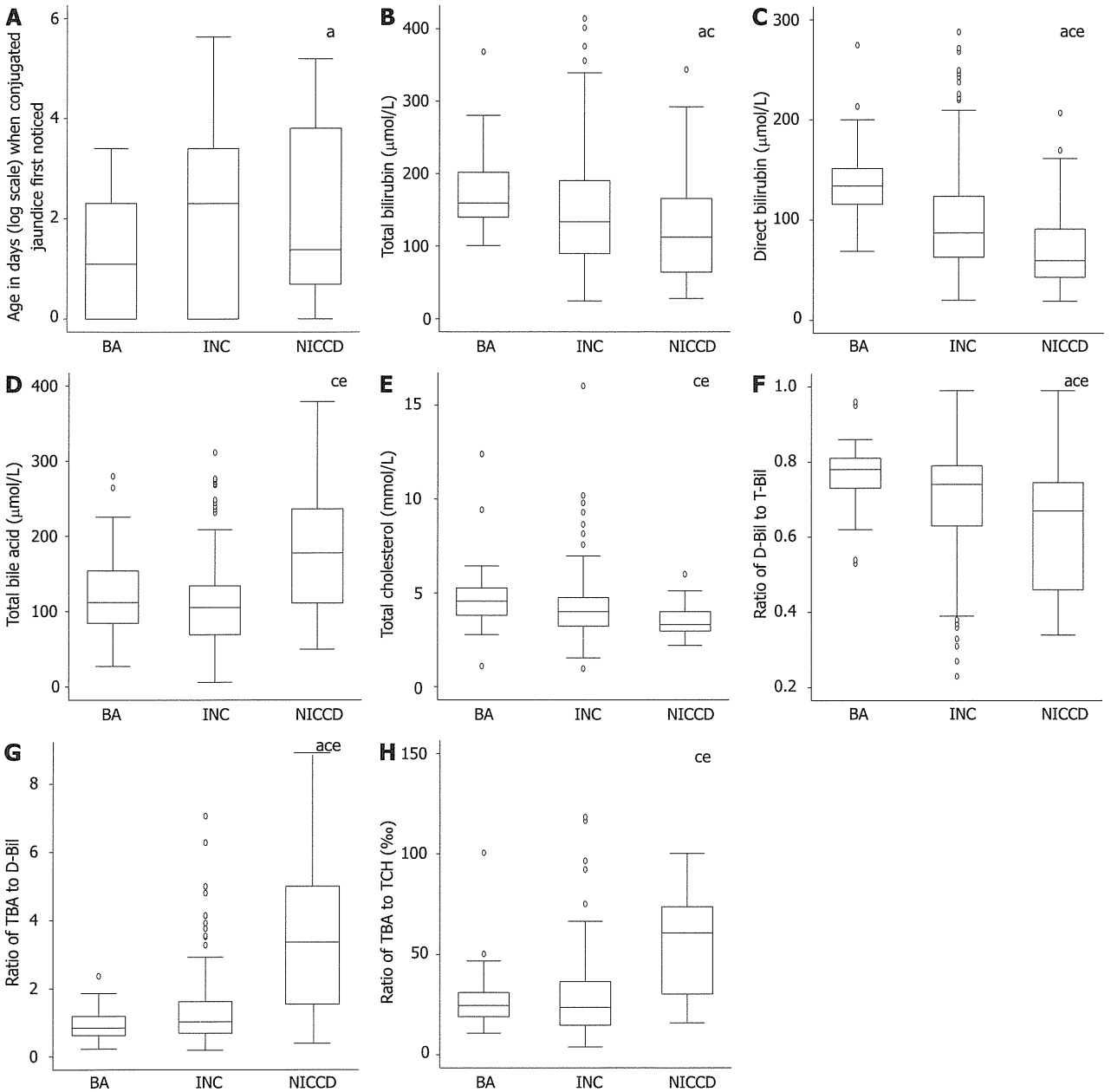

Figure 1 Comparison of the age when conjugated jaundice was first noticed (A), biochemistry indices (B-E), and ratios of some biochemical indices (F-H) in patients with neonatal intrahepatic cholestasis caused by citrin deficiency, idiopathic neonatal cholestasis and biliary atresia. $^{a}P < 0.05$ between BA and INC; $^{c}P < 0.05$ between BA and NICCD; $^{e}P < 0.05$ between INC and NICCD. Normal range: T-Bil (2-20 μmol/L), D-Bil (0-6 μmol/L), total bile acids (< 40 μmol/L), and TCH (3.12-5.20 mmol/L). NICCD: Neonatal intrahepatic cholestasis caused by citrin deficiency; BA: Biliary atresia; INC: Idiopathic neonatal cholestasis; TBA: Total bile acid; T-Bil: Total bilirubin; D-Bil: Direct bilirubin; TCH: Total cholesterol.

and that of NICCD 3.95 (3.36/0.85) times higher. For the ratio of TBA to cholesterol, if the median value of the BA group was taken as a standard, the median in the INC group was nearly the same as the standard but that in the NICCD group was 2.46 (60.7/24.7) times higher. These results indicate that the excretion of bile acids is much more severely affected than the excretion of bilirubin and cholesterol in NICCD patients. As a consequence, we may speculate that the failure to excrete bile acids from hepatocytes to the canalicula is the main mechanism of cholestasis caused by citrin deficiency.

The main limitation of this study was its retrospective nature. It could be argued that some biochemical indices were affected by the drugs that patients were taking. However, prior to the determination of a clear diagnosis, the management of patients had been similar in the three groups; therefore, the patients in the different groups would have been affected by these variables in the same way. Another measure that was used to avoid sample bias was using the first available laboratory data obtained when patients were referred to us. Although significant differences in TBA and TBA ratios were found between the NICCD and other two groups, no cut-off levels can be presented at this time.

COMMENTS

Background

Citrin deficiency is one of the most common metabolic disorders in Eastern Asia. It has at least two main phenotypes: neonatal intrahepatic cholestasis caused by citrin deficiency (NICCD) and adult-onset type II citrullinemia. The clinical features of and the mechanism of cholestasis in NICCD have yet to be established.

Research frontiers

Some biochemical indices of patients with NICCD have been compared to those of patients with biliary atresia (BA) and of patients with idiopathic neonatal cholestasis (INC). Comparison of these biochemical indices in neonatal cholestasis cases with different etiologies will better characterize the biochemical changes of the disease and may further the understanding of the mechanism of cholestasis caused by citrin deficiency.

Innovations and breakthroughs

Apart from confirming previous findings that NICCD patients had significantly lower alanine aminotransferase (ALT) level, lower direct bilirubin (D-Bil) to total bilirubin ratio, and significantly higher aspartate aminotransferase to ALT ratio compared to the BA and INC patients, this study specifically compared the serum level of total bile acid (TBA) and its ratio to D-Bil and cholesterol, and found that NICCD patients had significantly higher TBA levels as well as higher TBA to D-Bil and TBA to cholesterol ratios than patients with BA and INC.

Applications

The excretion of TBA appears to be much more severely disturbed than that of D-Bil and cholesterol in cholestasis caused by citrin deficiency. Further study of this condition will help elucidate the mechanism of cholestasis in NICCD, and the ratios could be further developed as indices for the differential diagnosis of neonatal cholestasis.

Peer review

The authors present an interesting retrospective study comparing liver specific biochemical parameters in different groups of infants with cholestasis.

REFERENCES

1 **Kobayashi K**, Sinasac DS, Iijima M, Boright AP, Begum L, Lee JR, Yasuda T, Ikeda S, Hirano R, Terazono H, Crackower MA, Kondo I, Tsui LC, Scherer SW, Saheki T. The gene mutated in adult-onset type II citrullinaemia encodes a putative mitochondrial carrier protein. *Nat Genet* 1999; **22**: 159-163

2 **Lu YB**, Kobayashi K, Ushikai M, Tabata A, Iijima M, Li MX, Lei L, Kawabe K, Taura S, Yang Y, Liu TT, Chiang SH, Hsiao KJ, Lau YL, Tsui LC, Lee DH, Saheki T. Frequency and distribution in East Asia of 12 mutations identified in the SLC25A13 gene of Japanese patients with citrin deficiency. *J Hum Genet* 2005; **50**: 338-346

3 **Song YZ**, Hao H, Ushikai M, Liu GS, Xiao X, Saheki T, Kobayashi K, Wang ZN. [A difficult and complicated case study: neonatal intrahepatic cholestasis caused by citrin deficiency]. *Zhongguo Dangdai Erke Zazhi* 2006; **8**: 125-128

4 **Yeh JN**, Jeng YM, Chen HL, Ni YH, Hwu WL, Chang MH. Hepatic steatosis and neonatal intrahepatic cholestasis caused by citrin deficiency (NICCD) in Taiwanese infants. *J Pediatr* 2006; **148**: 642-646

5 **Ko JS**, Song JH, Park SS, Seo JK. Neonatal intrahepatic cholestasis caused by citrin deficiency in Korean infants. *J Korean Med Sci* 2007; **22**: 952-956

6 **Thong MK**, Boey CC, Sheng JS, Ushikai M, Kobayashi K. Neonatal intrahepatic cholestasis caused by citrin deficiency in two Malaysian siblings: outcome at one year of life. *Singapore Med J* 2010; **51**: e12-e14

7 **Hutchin T**, Preece MA, Hendriksz C, Chakrapani A, McClelland V, Okumura F, Song YZ, Iijima M, Kobayashi K, Saheki T, McKiernan P, Baumann U. Neonatal intrahepatic cholestasis caused by citrin deficiency (NICCD) as a cause of liver disease in infants in the UK. *J Inherit Metab Dis* 2009 Jun 11; Epub ahead of print

8 **Dimmock D**, Maranda B, Dionisi-Vici C, Wang J, Kleppe S, Fiermonte G, Bai R, Hainline B, Hamosh A, O'Brien WE, Scaglia F, Wong LJ. Citrin deficiency, a perplexing global disorder. *Mol Genet Metab* 2009; **96**: 44-49

9 **Ohura T**, Kobayashi K, Tazawa Y, Nishi I, Abukawa D, Sakamoto O, Iinuma K, Saheki T. Neonatal presentation of adult-onset type II citrullinemia. *Hum Genet* 2001; **108**: 87-90

10 **Naito E**, Ito M, Matsuura S, Yokota T, Ogawa Y, Kitamura S, Kobayashi K, Saheki T, Nishimura Y, Sakura N, Kuroda Y. Type II citrullinaemia (citrin deficiency) in a neonate with hypergalactosaemia detected by mass screening. *J Inherit Metab Dis* 2002; **25**: 71-76

11 **Yamaguchi N**, Kobayashi K, Yasuda T, Nishi I, Iijima M, Nakagawa M, Osame M, Kondo I, Saheki T. Screening of SLC25A13 mutations in early and late onset patients with citrin deficiency and in the Japanese population: Identification of two novel mutations and establishment of multiple DNA diagnosis methods for nine mutations. *Hum Mutat* 2002; **19**: 122-130

12 **Yasuda T**, Yamaguchi N, Kobayashi K, Nishi I, Horinouchi H, Jalil MA, Li MX, Ushikai M, Iijima M, Kondo I, Saheki T. Identification of two novel mutations in the SLC25A13 gene and detection of seven mutations in 102 patients with adult-onset type II citrullinemia. *Hum Genet* 2000; **107**: 537-545

13 **Ohura T**, Kobayashi K, Tazawa Y, Abukawa D, Sakamoto O, Tsuchiya S, Saheki T. Clinical pictures of 75 patients with neonatal intrahepatic cholestasis caused by citrin deficiency (NICCD). *J Inherit Metab Dis* 2007; **30**: 139-144

14 **Tamamori A**, Okano Y, Ozaki H, Fujimoto A, Kajiwara M, Fukuda K, Kobayashi K, Saheki T, Tagami Y, Yamano T. Neonatal intrahepatic cholestasis caused by citrin deficiency: severe hepatic dysfunction in an infant requiring liver transplantation. *Eur J Pediatr* 2002; **161**: 609-613

15 **Shigeta T**, Kasahara M, Kimura T, Fukuda A, Sasaki K, Arai K, Nakagawa A, Nakagawa S, Kobayashi K, Soneda S, Kitagawa H. Liver transplantation for an infant with neonatal intrahepatic cholestasis caused by citrin deficiency using heterozygote living donor. *Pediatr Transplant* 2010; **14**: E86-E88

16 **Xing YZ**, Qiu WJ, Ye J, Han LS, Xu SS, Zhang HW, Gao XL, Wang Y, Gu XF. [Studies on the clinical manifestation and SLC25A13 gene mutation of Chinese patients with neonatal intrahepatic cholestasis caused by citrin deficiency]. *Zhonghua Yi Xue Yi Chuan Xue Zazhi* 2010; **27**: 180-185

17 **Song YZ**, Deng M, Chen FP, Wen F, Guo L, Cao SL, Gong J, Xu H, Jiang GY, Zhong L, Kobayashi K, Saheki T, Wang ZN. Genotypic and phenotypic features of citrin deficiency: five-year experience in a Chinese pediatric center. *Int J Mol Med* 2011; **28**: 33-40

18 **Dimmock D**, Kobayashi K, Iijima M, Tabata A, Wong LJ, Saheki T, Lee B, Scaglia F. Citrin deficiency: a novel cause of failure to thrive that responds to a high-protein, low-carbohydrate diet. *Pediatrics* 2007; **119**: e773-e777

19 **Tazawa Y**, Abukawa D, Sakamoto O, Nagata I, Murakami J, Iizuka T, Okamoto M, Kimura A, Kurosawa T, Iinuma K, Kobayashi K, Saheki T, Ohura T. A possible mechanism of neonatal intrahepatic cholestasis caused by citrin deficiency. *Hepatol Res* 2005; **31**: 168-171

20 **De Bruyne R**, Van Biervliet S, Vande Velde S, Van Winckel M. Clinical practice: neonatal cholestasis. *Eur J Pediatr* 2011; **170**: 279-284

21 **Wang JS**, Wang ZL, Wang XH, Zhu QR, Zheng S. The prognostic value of serum gamma glutamyltransferase activity in Chinese infants with previously diagnosed idiopathic neonatal hepatitis. *HK J Pediatr* 2008; **13**: 39-45

22 **Fu HY**, Zhang SR, Wang XH, Saheki T, Kobayashi K, Wang JS. The mutation spectrum of the SLC25A13 gene in Chinese infants with intrahepatic cholestasis and aminoacidemia. *J Gastroenterol* 2011; **46**: 510-518

23 **Fu HY**, Zhang SR, Yu H, Wang XH, Zhu QR, Wang JS. Most common SLC25A13 mutation in 400 Chinese infants with intrahepatic cholestasis. *World J Gastroenterol* 2010; **16**: 2278-2282

24 **Lee HC**, Mak CM, Lam CW, Yuen YP, Chan AO, Shek CC, Siu TS, Lai CK, Ching CK, Siu WK, Chen SP, Law CY, Tai HL, Tam S, Chan AY. Analysis of inborn errors of metabolism: disease spectrum for expanded newborn screening in Hong Kong. *Chin Med J* (Engl) 2011; **124**: 983-989
25 **Chen HW**, Chen HL, Ni YH, Lee NC, Chien YH, Hwu WL, Huang YT, Chiu PC, Chang MH. Chubby face and the biochemical parameters for the early diagnosis of neonatal intrahepatic cholestasis caused by citrin deficiency. *J Pediatr Gastroenterol Nutr* 2008; **47**: 187-192
26 **Tazawa Y**, Kobayashi K, Abukawa D, Nagata I, Maisawa S, Sumazaki R, Iizuka T, Hosoda Y, Okamoto M, Murakami J, Kaji S, Tabata A, Lu YB, Sakamoto O, Matsui A, Kanzaki S, Takada G, Saheki T, Iinuma K, Ohura T. Clinical heterogeneity of neonatal intrahepatic cholestasis caused by citrin deficiency: case reports from 16 patients. *Mol Genet Metab* 2004; **83**: 213-219
27 **Kimura A**, Kage M, Nagata I, Mushiake S, Ohura T, Tazawa Y, Maisawa S, Tomomasa T, Abukawa D, Okano Y, Sumazaki R, Takayanagi M, Tamamori A, Yorifuji T, Yamato Y, Maeda K, Matsushita M, Matsuishi T, Tanikawa K, Kobayashi K, Saheki T. Histological findings in the livers of patients with neonatal intrahepatic cholestasis caused by citrin deficiency. *Hepatol Res* 2010; **40**: 295-303

S- Editor Lv S **L- Editor** Kerr C **E- Editor** Lu YJ

Journal of Neurochemistry

JOURNAL OF NEUROCHEMISTRY | 2013 | 124 | 347–362 doi: 10.1111/jnc.12096

ORIGINAL ARTICLE

AGC1-malate aspartate shuttle activity is critical for dopamine handling in the nigrostriatal pathway

Irene Llorente-Folch,* Ignasi Sahún,† Laura Contreras,* María José Casarejos,‡ Josep María Grau,§ Takeyori Saheki,¶ María Angeles Mena,‡ Jorgina Satrústegui,* Mara Dierssen† and Beatriz Pardo*

*Departamento de Biología Molecular, Centro de Biología Molecular Severo Ochoa UAM-CSIC, and CIBER de Enfermedades Raras (CIBERER), Universidad Autónoma de Madrid, Madrid, Spain

†Programme of Genes and Disease, Center for Genomic Regulation, and CIBER de Enfermedades Raras (CIBERER), Barcelona, Spain

‡Department of Neurobiology and CIBERNED, Hospital Ramón y Cajal, Carretera de Colmenar km 9,1, Madrid, Spain

§Department of Internal Medicine and Pathology, Hospital Clinic, University of Barcelona Medical School, Barcelona, Spain

¶Institute of Resource Development and Analysis, Kumamoto University 2-2-1 Honjo, Kumamoto, Japan

Abstract

The mitochondrial transporter of aspartate-glutamate Aralar/AGC1 is a regulatory component of the malate-aspartate shuttle. Aralar deficiency in mouse and human causes a shutdown of brain shuttle activity and global cerebral hypomyelination. A lack of neurofilament-labeled processes is detected in the cerebral cortex, but whether different types of neurons are differentially affected by Aralar deficiency is still unknown. We have now found that Aralar-knockout (Aralar-KO) post-natal mice show hyperactivity, anxiety-like behavior, and hyperreactivity with a decrease of dopamine (DA) in terminal-rich regions. The striatum is the brain region most affected in terms of size, amino acid and monoamine content. We find a decline in vesicular monoamine transporter-2 (VMAT2) levels associated with increased DA metabolism through MAO activity (DOPAC/DA ratio) in Aralar-KO striatum. However, no decrease in DA or in the number of nigral tyrosine hydroxylase-positive cells was detected in Aralar-KO brainstem. Adult Aralar-hemizygous mice presented also increased DOPAC/DA ratio in striatum and enhanced sensitivity to amphetamine. Our results suggest that Aralar deficiency causes a fall in GSH/GSSG ratio and VMAT2 in striatum that might be related to a failure to produce mitochondrial NADH and to an increase of reactive oxygen species (ROS) in the cytosol. The results indicate that the nigrostriatal dopaminergic system is a target of Aralar deficiency.

Keywords: AGC-1 deficiency, dopamine, global cerebral hypomyelination, malate-aspartate shuttle, OmniBank®, VMAT2.

J. Neurochem. (2013) **124**, 347–362.

Aralar is the brain isoform of the mitochondrial transporter of aspartate/glutamate mainly expressed in neurons (Del Arco and Satrústegui 1998; Ramos *et al.* 2003; Pardo *et al.*

Abbreviations used: 3-MT, 3-methoxy-tyramine; 5-HT, serotonin; AGC1, aspartate-glutamate carrier; COMT, catechol-*ortho*-methyl-transferase; DA, dopamine; DARPP32, dopamine and cAMP regulated phosphoprotein of 32 KDa; DAT, dopamine transporter; DOPAC, 3,4 dihydroxy-phenyl acetic acid; GSH, reduced glutathione; GSSG, oxidized glutathione; HVA, homovanillic acid; MAO, monoamine oxidase; MAS, malate-aspartate shuttle; NAA, N-acetylaspartate; NA, noradrenaline; PD, Parkinson's disease; PND, post-natal day; ROS, reactive oxygen species; SERT, serotonin transporter; TH, tyrosine hydroxylase; Tyr, tyrosine; VMAT2, vesicular monoamine transporter 2.

Received August 3, 2012; revised manuscript received October 9, 2012; accepted November 5, 2012.

Address correspondence and reprint requests to Beatriz Pardo, Centro de Biología Molecular Severo Ochoa UAM-CSIC, and CIBER de Enfermedades Raras (CIBERER), Universidad Autónoma de Madrid, 28049-Madrid, Spain. E-mail: bpardo@cbm.uam.es

2006, 2011) and its expression is increased during maturation in parallel to malate-aspartate shuttle (MAS) activity (Ramos *et al.* 2003). Aralar deficiency leads to a loss of respiration on malate plus glutamate, a shutdown of MAS activity, and a drop in brain and neuronal aspartate levels (Jalil *et al.* 2005). Neurons from Aralar-KO mice have a clear metabolic impairment in glucose oxidation because of the lack of a functional MAS, which results in lower pyruvate levels and increased lactate production (Pardo *et al.* 2011). In intact cultured neurons, the maximal respiratory capacity of Aralar-KO neurons is clearly reduced as compared with control (Gómez-Galán *et al.* 2011), reflecting the limitation in pyruvate supply to mitochondria in the absence of a functional MAS. Other NADH shuttle systems, as the glycerophosphate shuttle (GPS) may partially compensate for the lack of Aralar. Indeed, although GPS was thought to be non-functional in neurons and astrocytes which lack the major isoform of cytosolic glycerophosphate dehydrogenase (Nguyen *et al.* 2003), the mRNA of a second cytosolic glycerol-P-dehydrogenase (GPD1-like), functionally identified in heart (Liu *et al.* 2010), is expressed in neurons and astrocytes (Cahoy *et al.* 2008). However, even if GPS exerts some compensation, it is unable to prevent the limitation in pyruvate supply caused by Aralar deficiency.

Aralar-KO mice show a drop of N-acetylaspartate (NAA), hypomyelination, and a progressive failure to synthesize glutamine in brain astrocytes, suggesting that glutamatergic neurotransmission may be compromised in the older animals (Jalil *et al.* 2005; Pardo *et al.* 2011). These mice present motor problems, tremor, seizures, and premature death (Jalil *et al.* 2005). Impaired development or degeneration of neuronal processes unrelated to myelin deficits has been observed in Aralar-KO mouse brain (Ramos *et al.* 2011). Recently, a patient with an homozygous loss of function mutation in *SLC25A12* was reported to show a loss of mitochondrial respiration on malate plus glutamate, low NAA levels, hypomyelination, arrested psychomotor development, hypotonia, and seizures (Wibom *et al.* 2009). These findings are relevant as the main features of Aralar deficiency (reduced NAA levels and hypomyelination) are common in mouse and human, and support the importance of the Aralar-KO mouse for the study of the global cerebral hypomyelination (OMIM ID #612949). To gain further insight into the behavioral deficits of the Aralar-KO mouse, in comparison with human AGC-1 deficiency, we have studied in more detail motor abilities and general behavior in Aralar-KO mice from post-natal day 13 (PND13) to PND20. In addition, we have analyzed neurochemical changes in specific brain areas of the Aralar-KO mouse that could be responsible for the behavioral failures observed. Further studies have been performed on healthy and adult mice expressing only half-a-dose Aralar.

Our data indicate that Aralar-KO mice show deficits in motor coordination, ataxic gait, increased reactivity, hyperactivity, and anxiety-like behavior, together with a pronounced decline in the striatal levels of DA. Besides, both PND20 Aralar-KO and 18-month-old Aralar-hemizygous mice display DA mishandling in striatum. The present results reveal a high susceptibility of DAergic neurons, specifically those DAergic groups of the nigrostriatal system, to Aralar-MAS dysfunction. A large body of evidence supports that nigrostriatal DAergic neurons are highly vulnerable to oxidative stress (Mena *et al.* 1993, 1997, 2002; Pardo *et al.* 1995; Canals *et al.* 2001), and to impairments of energy metabolism (Zeevalk *et al.* 1997; Watabe and Nakaki 2008; Pickrell *et al.* 2011; Sterky *et al.* 2012). Our results evidence that the striatum is a preferential target of Aralar deficiency which leads to a reduction and/or mishandling of DA and suggest a role of oxidative stress caused by Aralar deficiency as the origin of DA mishandling in striatum.

Materials and methods

Methods including histological and immunohistochemical studies in brain and histomorphological studies of muscle are described in Supplementary material.

Animals

Male SVJ129 x C57BL6 mice carrying a deficiency for ARALAR expression (Aralar wild-type, WT; Aralar heterozygous, HT; and Aralar Knock-out, KO) were obtained from Lexicon Pharmaceuticals, Inc. (The Woodlands, TX, USA) (1). The mice were housed in a humidity- and temperature-controlled room on a 12-h light/dark cycle, receiving water and food *ad libitum*. Genotype was determined by PCR using genomic DNA obtained from tail or embryonic tissue samples (Nucleospin tissue kit; Macherey-Nagel, Düren, Germany) as described previously (Jalil *et al.* 2005). All the experimental protocols used in this study were approved by the local Ethics Committees at the Center of Molecular Biology 'Severo Ochoa', Autónoma University (UAM), Madrid, and at the Center for Genomic Regulation, Barcelona.

General procedure for post-natal observations

All the pregnant females were allowed to deliver spontaneously. Each pup was checked for gross abnormalities and the day after delivery was designated as PND1 of age for neonates (estimation error on time of birth ± 8 h). The pups were individually marked with ink and were nursed by their natural dams until weaning. During the testing protocol, whole litters were separated from the dam less that 10 min and maintained in a warm environment. Males and females were pooled to perform the neurodevelopmental screening. All the measures were performed between 5:00 a.m. and 8:00 a.m. All experiments procedures were approved by the Animal Care Committee of the Centre for Genomic Regulation. For the developmental screening 42 animals, males and females, were employed from five different litters.

Neurobehavioral development

Reflex and sensory function

Visual placing. After the opening of the eyes, the pup was suspended by the tail and lowered toward the tip of a pencil without the vibrissae touching it, on PND17. The response was considered positive when the paws were extended to touch it.

Blast response. Exaggerated jumping or running behavior in response to a gentle puff of air, on PND11.

Tactile orientation. The test assessed the head turning (orienting) response triggered by the application to one side of the perioral area a cotton Q-tip, beginning on PND11.

Vibrissae orientation. The pups were suspended by the tail and lowered toward the tip of a cotton Q-tip. At contact of the cotton with the vibrissae, the pup raised its head and performed a placing response, beginning on PND8.

Preyer reflex/startle response. The response of the pups to a moderate sound burst consisting of a moderately brink flick of the pinna or startle response was recorded, beginning on PND11.

Toe pinch. The test assessed the presence or absence of withdrawal answer against a mild painful stimulus, exerting pressure in a hind paw with the fingers, on PND17.

Reaching response. The animal is held by the tail above a flat surface and it is noted if the forepaws are stretched out to make contact with the surface, on PND17.

Touch escape. Response of the animal to a finger stroke from above was recorded and scored, beginning on PND13, as follow: 0 = no response, 1 = moderate (rapid response to light stroke); and 2 = vigorous (escape response to approach).

Homing test

On PND19, individual pups were transferred to a cage containing new sawdust with a bite portion of sawdust of the home litter 'goal arena'. The pups were located at the opposite side of the goal arena, near to the wall. The time taken to reach the home litter sawdust was recorded (cut-off time 60 s).

Paw print test

To examine the step patterns of the hind limbs during forward locomotion, mice were required to traverse a straight, narrow tunnel. The experiments to evaluate the walking pattern of the mice were adapted from previous study by Martínez de Lagrán *et al.* (2004) and performed on PND18. The hind paws of the pups were coated with blue non-toxic waterproof ink. Animals were then placed at one end of a long narrow tunnel (10 × 10 × 30 cm), and in the opposite end there were placed part of their nest. They spontaneously enter and partially or totally traverse the tunnel. A clean sheet of white paper was placed on the floor of the tunnel to record the paw prints. The pattern of three consecutive steps (the first four steps were excluded from the analysis) was analyzed and the following parameters assessed, averaged over consecutive steps: (i) stride length, the averaged distance between each stride; (ii) hindpaw base width, measured as the average distance between left and right hind footprint overlap. These values were determined by measuring the perpendicular distance of a given step to a line connecting its opposite preceding and proceeding.

Beam balance test

On PND19, individual pups were located in a trip of 40 × 2 cm elevated 25 cm from the surface. They began the task in the middle of the wooden trip and they should travel to reach the end of the trip with a cut-off time of 60 s. Latency to the first movement, arrival latency and latency to fall were recorded. There was a first training session where the animals performed the task and learned about the mechanism. Mice were guided along the trip holding them by the tail to avoid any fall if they were not able to do it themselves. In a period of an hour the test was repeated, in this case without any help and counting the times.

Open field test

The open field was a white melamine box (70 × 70 × 50 cm high) divided into 25 equal squares and under high intensity light levels (lighted, 500 Lux) or in darkness (with weak red light). Mice tend to avoid brightly illuminated, novel, open spaces, so the open field environment acts as an anxiogenic stimulus and allows for measurement of anxiety-induced locomotor activity and exploratory behavior s. Thus, two zones, center (1764 cm^2) and periphery (3136 cm^2) were delineated, being the center more anxiogenic. At the beginning of the test session, mice at PND15–16 were left in the periphery of the apparatus and during 5 min we measured and analyzed the latency to cross from the periphery to the center, total distance traveled, average speed and time spent in several sectors of the field (i.e., the border areas vs. the open, central area). Observation was made in an actimeter (Panlab, Barcelona, Spain) by computerized analysis of movements.

To test the actively behavioral effect of amphetamine in 18-month-old Aralar mice (Aralar- WT and Aralar-HT, $n = 7$), we performed an acute intraperitoneal administration protocol using three different drug concentrations: 1.5, 3.0, and 5.0 mg/kg, and saline as a control (sham). Aging animals performed the task immediately after the amphetamine treatment and developed the task once every other day increasing the drug dose concentration. Locomotor activity was measured in actimetry boxes (45 × 45 cm; Harvard Apparatus, Panlab) and movements on the ground were monitored via a grid of infrared beams and used as an index of locomotor activity (counts). All data were collected with Acti-Track software (Harvard Apparatus).

Statistical analysis

For behavioral and motor tests, variance homogeneity and normality of data were tested by means of Levene and Shapiro–Wilk tests, respectively. Simple comparisons between genotypes mice were performed using the two-tailed unpaired Student's *t*-test with Whitney's correction to account for the different variances in the populations being studied. If the data did not meet specifications required for parametric analysis, non-parametric analysis of variance was used (Kruskal–Wallis) followed by comparisons between groups (Mann–Whitney *U*-test). Data were expressed as mean F SEM. In all tests, a difference was considered significant if the

obtained probability value was $p < 0.05$. These statistical analyses were performed with the commercial software package Statistica 7.0 (StatSoft, Tulsa, OK, USA).

Brain regions and tissue preparation for amino acid analysis

Mice at PND19 were anesthetized, the whole brain was immediately removed from the skull and the brain regions were dissected according to Carlsson and Lindqvist (1973) and Itier *et al.* (2003) into the DA-rich limbic portion, the corpora striata (striatum), diencephalon, brainstem, cerebellum, and cerebral cortex. Regions were sonicated in 3% perchloric acid (PCA), neutralized, and centrifuged at 10 000 *g* for 15 min. Supernatants were lyophilized and dissolved in 0.2 M lithium citrate loading buffer pH 2.2 for quantification with an automatic amino acid analyzer Biochrom 20 (Pharmacia, Uppsala, Sweden) using a precolumn derivatization with ninhydrin and a cationic exchange column.

Measurements of monoamines in selected brain regions

The levels of DA and its metabolites, 3-methoxy-tyramine (3-MT), 3,4 dihydroxy-phenyl acetic acid (DOPAC) and homovanillic acid (HVA), noradrenaline (NA) and its metabolite, 4-hydroxy-3-methoxy-phenyl-glycol (MHPG), serotonin (5-HT) and its metabolite, 5-hydroxy-indole-acetic acid (5-HIAA) were measured by HPLC with an ESA coulochem detector, according to Mena *et al.* (1995). Briefly, samples from the same brain regions indicated above were sonicated in 8 volumes (w/v) of 0.4 N perchloric acid (PCA) with 0.5 mM $Na_2S_2O_5$ and 2% EDTA and then centrifuged for 10 min. Monoamine levels were determined from 20 uL of the supernatant. The chromatographic conditions were as follows: a column Nucleosil 5C18; the mobile phase, a 0.1 M citrate/acetate buffer, pH 3.9 with 10% methanol, 1 mM EDTA and 1.2 mM heptane sulfonic acid; and the detector voltage conditions: D1 (+0.05), D2 (−0.39), and the guard cell (+0.4).

Measurements of glutathione in brain regions

Total glutathione (Gsx) levels were measured by the method of Tietze (1969). A sample (40 μL) of the sonicated brain region supernatant in 0.4 N PCA was neutralized with four volumes of phosphate buffer (0.2 M NaH_2PO_4, 0.2 M Na_2HPO_4, 0.5 M EDTA, and pH 7.5). Fifty microliters of this preparation were mixed with 5,5′-dithiobis-(2-nitrobenzoic acid) (0.6 mM), NADPH (0.2 mM), and glutathione reductase (1 unit) and the reaction was monitored in a P96 automatic microtiter reader at 412 nm for 6 min. Oxidized glutathione (GSSG) was measured as described by Griffith (1980). After the neutralization with the phosphate buffer, the sample remaining was mixed with 2-vinylpyridine (1.2 μL) at 25°C for 1 h and the reaction was carried out as described earlier. Reduced glutathione (GSH) was obtained by subtracting GSSG levels from Gsx levels.

Western blot in brain tissue

Aliquots (20 μg of protein) of brain lysates (in 20 mM Tris-HCl, 10 mM AcK, 1 mM dithiothreitol , 1 mM EDTA, protease inhibitor cocktail tablet (complete Mini, EDTA-free; Roche Diagnostics, Mannheim, Germany) 0.25% NP-40, pH 7.4) were centrifuged (12 000 *g*, 30 min at 4°C) and electrophoresed in an 8% sodium dodecyl sulfate acrylamide gel. Proteins were transferred electrophoretically to nitrocellulose membranes, which were blocked in 5% (w/v) dry skimmed milk (Sveltesse, Nestle) in Tris-buffered saline (10 mM Tris-HCl pH 7.5, 150 mM NaCl plus 0.05% (v/v) Tween-20) for 2 h, and further incubated with antibodies against Aralar (Del Arco and Satrústegui 1998) (polyclonal antibody, 1 : 1000), dopamine markers (tyrosine hydroxylase, TH polyclonal antibody Millipore (Billerica, MA, USA), 1 : 5000; dopamine transporter, DAT (SLC6A3) monoclonal antibody Millipore, 1 : 2000; vesicular monoamine transporter, VMAT2 (SLC18A2) polyclonal antibody Millipore 1 : 1000; dopamine and adenosine 3′, 5′-monophosphate-regulated phosphoprotein (32 kDa), DARPP-32 polyclonal antibody Millipore 1 : 10 000), GABAergic marker [glutamic acid decarboxylase (GAD)65, Chemicon (Caramillo, CA, USA), polyclonal antibody, 1 : 1000], glial markers [GFAP polyclonal antibody Dakopatts (Glostrup, Germany) 1 : 500, for astrocytes; and OX-6 monoclonal antibody Serotec (Kidlington, UK) 1 : 500, for microglia], and β-actin (monoclonal antibody Sigma (St Louis, MO, USA), 1 : 10 000), for 1 h at 25°C. Signal detection was performed with and enhanced chemiluminescence substrate (Western lighting-ECL; PerkinElmer, Baesweiler, Germany).

Statistical analysis

For biochemical data, the statistical significance of the differences was assessed by One-way analysis of variance (ANOVA) followed by a *post hoc* Student's, Duncan/Tukey or Student-Newman-Keuls *t*-test method, as indicated. The results are expressed as mean ± standard error of the mean (SEM).

Results

Hyper-reactivity, demotivation, and motor discoordination are observed in Aralar-KO mice

A battery of behavioral and motor tests was carried out to elucidate the specific problems related to AGC1-MAS deficiency. When performing the toe pinch test, Aralar-KO mice presented hyper-reactivity as compared to WT mice (Fig. 1b), with no alteration in other sensory functions (i.e., visual placing, blast response, tactile and vibrissae orientation; not shown). Gross postural alterations became evident in Aralar/AGC1 KO mice analyzing the reaching response capacity (Fig. 1a). Aralar-KO animals showed a limb clasping phenotype, instead of showing a normal escape posture. Hyper-reactivity could also explain the results obtained in the touch escape test (Fig. 1d), where KO mice showed an exacerbated response to a finger stroke from above with no aversive effect in Aralar-WT or Aralar-hemizygous (HT) littermates.

To evaluate the psychomotor state, social behavior and motivations, we performed the homing test (Fig. 1c). The latency of Aralar wild-type (WT) mice to reach the opposite side of the cage stimulated by the presence of the nest was 7.2 ± 1.3 s, showing high motivation to reach the goal. In contrast, Aralar-KO mice did not show any displacement toward the target during the test. As the motor activity, measured in the open field test (Fig. 1e–g), seemed to be intact in Aralar-KO mice, the phenotype observed in the homing test may reflect demotivation and/or inability to

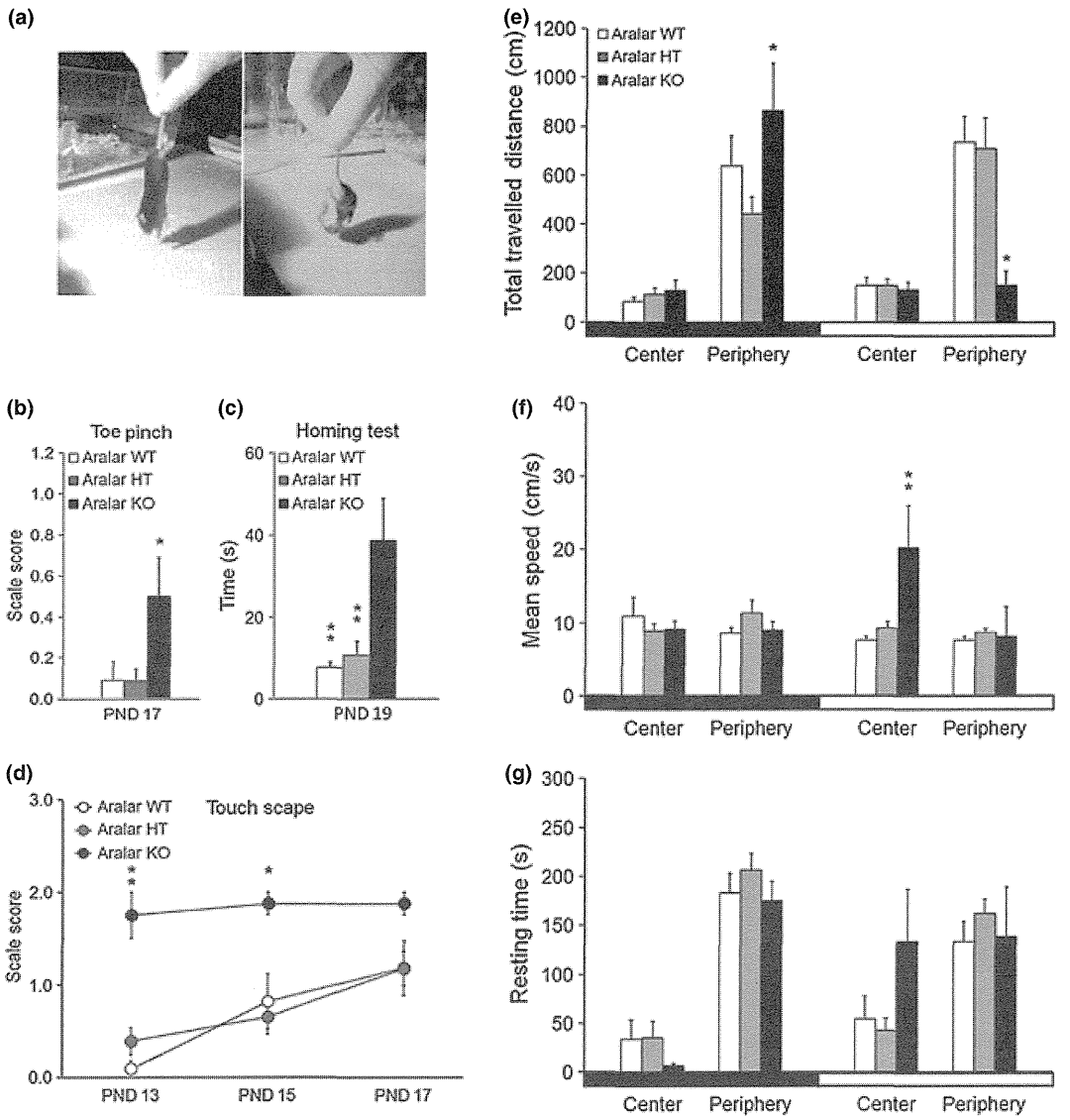

Fig. 1 Hyperreactivity, hyperactivity, and social impairments in Aralar-knock-out (KO) mice. Reaching response (a) and toe pinch at post-natal day (PND)17 (b), homing test (c, denoting exploratory, social, and motor behavior) and touch scape (d) are illustrated in wild-type (open circles or bars), Aralar-hemizygote (gray circles or bars) and Aralar-KO mice (filled circles or bars). (e–g) Open field studies show high levels of hyperactivity and anxiety-like behavior in Aralar-KO mice. Parameters as total traveled distance (e), mean speed of walk (f) and resting time between displacements (g) in the center and periphery of the arena and at darkness (basal)-light (aversive) conditions are valutated in wild-type (WT), Aralar-hemizygote, and Aralar-KO mice. In (b and d) non-parametric analysis of variance was used (Kruskal–Wallis) followed by comparisons between groups (Mann–Whitney *U*-test). Simple comparisons between genotypes mice were performed in (c) using the two-tailed unpaired Student's *t*-test with Whitney's correction. One-way ANOVA with Bonferroni test for *post hoc* analyses was performed in open field test. Data are expressed as the mean ± SEM (n = 8–13 mice per group). $*p \leq 0.05$, $**p \leq 0.01$, $***p \leq 0.001$.

initiate a voluntary motor response, one of the signs of basal ganglia dysfunction, particularly involving the caudate-putamen (Hauber 1998; Palmiter 2008).

The results of the pawprint analysis showed a gait disturbance in Aralar-KO mice (Fig. 2a and b). KO mice exhibited a significantly shorter stride length and hindpaw base width than their WT littermates (Fig. 2a), according to their smaller size, additionally presenting an erratic direction of path and in-coordination (Fig. 2b). Beam balance test clearly demonstrated a motor impairment of Aralar-KO mice (Fig. 2c) who tended to lock in a fixed spastic posture while on the beam and almost all Aralar-KO mice fell off the bar. The delayed onset for the first movement in KO mice on the bar is near the maximum latency estimated in the task, 60 s, while WT mice improved the performance in the second trial starting the movement in 26.5 ± 7.8 s and reaching the end of the beam in 29.3 ± 7.5 s. These motor deficits could be attributable to striatal dysfunction (Menéndez *et al.* 2006;

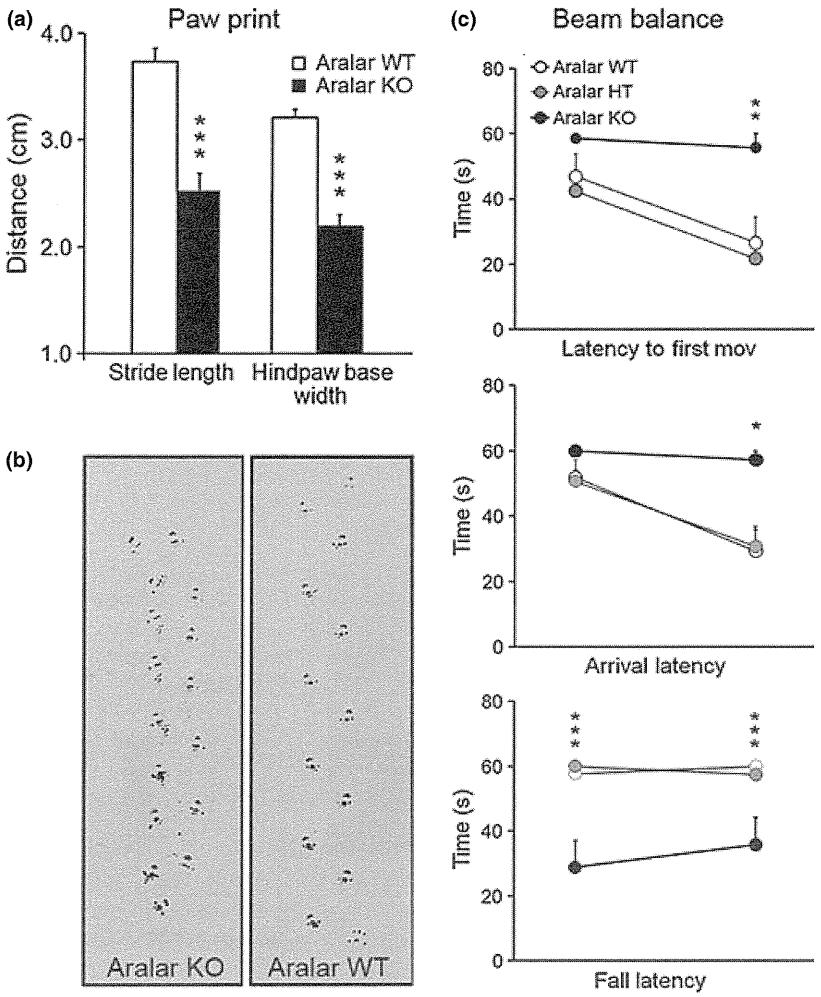

Fig. 2 Aralar-knock-out (KO) mice have a dramatic motor discoordination. In the pawprinting test (a, b) it is noticeable that Aralar-KO mice have a shorter stride length and a shorter hindpaw length than the wild-type (WT) siblings (a), and an erratic direction of walk (b). Asymmetric gait at the right leg is shown in the footprint left by the hind limbs of Aralar-KO mice walking on the paper (b). The beam balance test (c) was performed in wild-type (open circles), Aralar-hemizygote (gray circles), and Aralar-KO mice (filled circles). 1 and 2 indicates the number of assay. Statistical analysis was performed by two-tailed unpaired Student's *t*-test with Whitney's correction. Data are expressed as the mean ± SEM (n = 10–13 mice per group). $*p \leq 0.05$, $**p \leq 0.01$, $***p \leq 0.001$.

Taylor *et al.* 2011) or increased anxiety/fear-related responses.

Thus, KO mice showed a lack of motor coordination in the hindlimbs with no muscle affectation (Figure S1), indicating a failure in midbrain and/or forebrain structures.

Enhanced locomotor, exploratory activity, and emotionality in Aralar-KO mice

The open field test, used to study spontaneous locomotor activity and anxiety-related behavior in mouse (Carola *et al.* 2002), was assessed in two different environments, in darkness less aversive conditions (with red light) and in lighted aversive conditions (Fig. 1e–g). Both WT and Aralar-KO were able to perform properly the task at PND15–16. Total distance traveled in darkness was statistically higher in Aralar-KO, with strong thigmotaxic behavior (preference to the periphery), compared with WT mice (Fig. 1e), indicating a more anxious-like behavior. Aralar-KO mice were as fast as WT (mean speed, 8.7 ± 0.9 cm/s; Fig. 1f), but with lower resting time (Fig. 1g) indicating hyperactivity. In the aversive (lighted) condition, Aralar-KO mice traveled significantly less distance in periphery than WT and than they did in darkness conditions (Fig. 1e). Moreover, they showed a striking burst of speed in the center of the arena (Fig. 1f). Grooming and fecal boli in the lighted versus. darkness condition were equally increased in all mice, however, the vertical activity (rearing), which involves hindlimb strength, tended to be higher in Aralar-KO mice in darkness condition than in WT mice (not shown), and this is also consistent with hyperactivity. These results indicate a rise in anxiety-, emotionality-related behavior s and reactivity in Aralar-KO animals.

Striatum is the main target for AGC1 deficiency

Although expression of Aralar-AGC1 has been extensively reported to be mainly restricted to and highly expressed in brain neurons (Ramos *et al.* 2003; Berkich *et al.* 2007; Xu *et al.* 2007; Cahoy *et al.* 2008; Pardo *et al.* 2011), no neuronal cell death in brain from Aralar-KO mice was detected (not shown), but evident hypomyelination and loss of neurofilaments was reported occurring in specific brain regions (Jalil *et al.* 2005; Sakurai *et al.* 2010; Ramos *et al.*

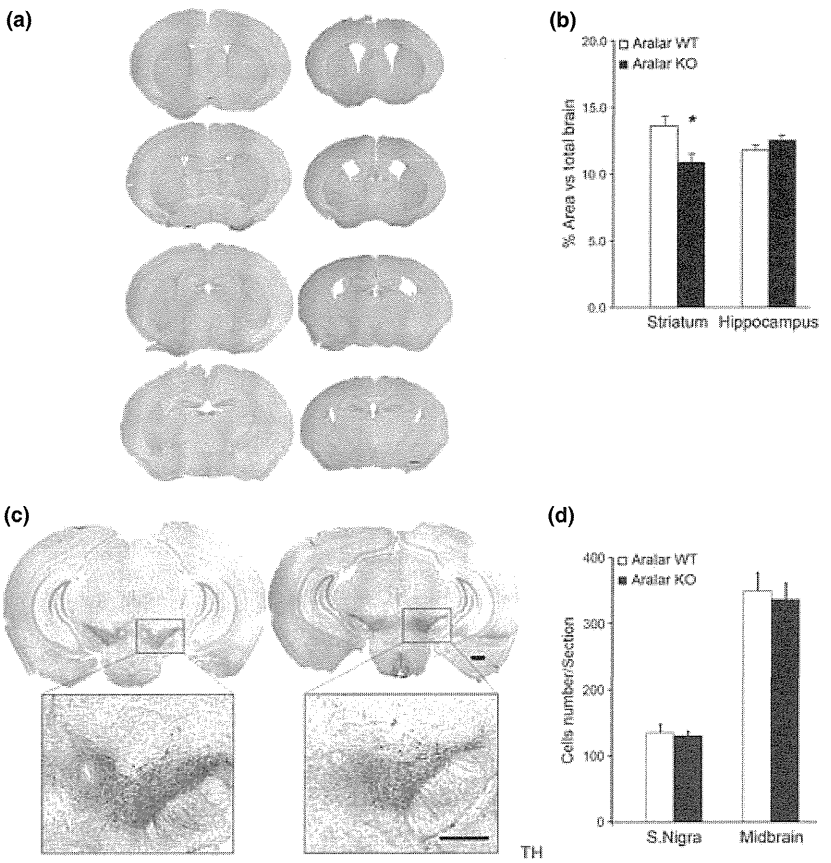

Fig. 3 Aralar-knock-out (KO) mice show no morphological abnormalities in brain, but an enlargement in lateral ventricule and a reduction in size of striatum. View of coronal sections are shown stained with cresyl violet in wild-type (wt) and Aralar-KO animals at post-natal day (PND)20 (scale bar, 500 μm) (a). (b) Quantitation of the area for striatum and hippocampus versus that of whole brain is represented, as percentage, in Aralar-WT (open bars) and Aralar-KO mice (filled bars; $n = 4$). (c) View of coronal sections of the brain from WT and Aralar-KO mice at PND20 as observed at the high power (scale bar, 500 μm), ($n = 6$ mice). (d) The number of positive-neurons for tyrosine hydroxylase (TH) in the *substantia nigra* (SN) and *midbrain* was found to be equal in Aralar-KO as compared with control mice. Statistical analysis was performed by two-tailed unpaired Student's *t*-test with Whitney's correction. Data are expressed as the mean ± SEM $^*p \leq 0.05$.

2011). Aralar-KO mice have brain abnormalities consisting of a marked enlargement in brain lateral ventricles (Fig. 3a) (Jalil *et al.* 2005), also reported in human AGC-1 deficiency (Wibom *et al.* 2009). Figure 3 shows that the enlargement of lateral ventricles is related to a reduction in the size of striatum. Thus, the striatum/brain ratio size was significantly reduced to 80% in Aralar-KO mice versus WT (13.33 ± 0.04% and 10.76 ± 0.03% in WT and Aralar-KO, respectively; $p = 0.0286$), while the hippocampus/brain ratio size was unchanged (11.77 ± 0.02 and 12.74 ± 0.02% in WT and Aralar-KO, respectively; Fig. 3b). Interestingly, the AGC1-deficient patient has also a smaller caudate-putamen than expected (Wibom *et al.* 2009).

Consistent with a preferential effect of Aralar deficiency in striatum, we found that the drop in whole brain Glutamine content previously reported (Pardo *et al.* 2011) is more prominent in the striatum (Table 1) than in all the other brain regions analyzed, reaching 29% of WT levels in Aralar-KO mice. However, in cerebellum and particularly in brainstem Glutamine levels hardly drop (in cerebellum to 82% of WT levels, $p < 0.05$; and no change in brainstem) perhaps because of the presence of low levels of citrin, a component of malate-aspartate shuttle homologous to Aralar, in these brain areas (Contreras *et al.* 2010). Striatal GABA was also significantly reduced to 60% in Aralar-KO (Table 1), with no changes in all the other brain regions.

On the other hand, Table 1 shows that none of the brain regions analyzed differed with respect to the drop in whole brain aspartate, serine and alanine levels (Pardo *et al.* 2011). Thus, the striatum appeared to be the brain region most affected by aralar deficiency.

Monoamine metabolism is impaired in brain from Aralar-deficient mice

Given the marked inability of Aralar-KO mice to perform motor tasks and the hyper-reactivity, hyper-activity, and anxiety observed in the tests performed, and the prominent effect of Aralar deficiency in the striatum, we decided to investigate the metabolism of monoamines in several brain regions, and particularly in striatum, as it is closely involved in the former functions (see Stein *et al.* 2006 for references).

NA content was similar in WT and Aralar-KO mice in any of the regions studied (Table 2).

Regarding the serotoninergic system, Aralar deficiency resulted in a significant decrease both in 5-HT levels and specially those of its intracellular degradation product 5-HIAA in diencephalon (to 51% and 43%, respectively, vs. control) and brainstem (to 72% and 59%, respectively) (Table 2), with similar changes (not always significant) in

Table 1 Amino acid content in brain extracts from Aralar-WT mice and Aralar-KO mice at 20 days (striatum, diencephalon, hipocampus, brainstem, cerebral cortex, and cerebellum)

Aminoacids (nmol/g tissue)		Striatum	Diencephalon	Limbic system	Brain stem	Cer. Cortex	Cerebellum
Aspartate	AralarWT	2264 ± 175	2466 ± 122	1894 ± 232	2409 ± 156	2356 ± 91	2379 ± 62
	Aralar KO	454 ± 41***	429 ± 21***	399 ± 48**	562 ± 34***	430 ± 54***	706 ± 61***
	(% vs WT)	20%	17%	21%	23%	18%	29%
Serine	AralarWT	1101 ± 90	790 ± 74	1014 ± 159	514 ± 19	1000 ± 33	709 ± 48
	Aralar KO	160 ± 16***	164 ± 13**	138 ± 9**	168 ± 26***	196 ± 24***	215 ± 18**
	(% vs WT)	14%	21%	13.6%	33%	20%	30%
Alanine	AralarWT	783 ± 97	573 ± 39	870 ± 128	525 ± 18	805 ± 22	497 ± 19
	Aralar KO	297 ± 63**	180 ± 18***	211 ± 15**	238 ± 36***	261 ± 23***	201 ± 19***
	(% vs WT)	38%	31%	24%	45%	32%	40%
Glutamate	AralarWT	7512 ± 487	7615 ± 321	8166 ± 1076	5840 ± 258	8326 ± 252	8071 ± 237
	Aralar KO	4030 ± 238**	3935 ± 230***	4446 ± 577**	4141 ± 235**	5797 ± 575**	5202 ± 418***
	(% vs WT)	54%	52%	54.4%	71%	70%	64%
Glutamine	AralarWT	3019 ± 258	2880 ± 143	2548 ± 301	2653 ± 205	2449 ± 231	3808 ± 143
	Aralar KO	895 ± 166***	1387 ± 233**	1133±268**	2569 ± 185	1471 ± 264**	3119 ± 352*
	(% vs WT)	29%	48%	44.4%	–	60%	82%
GABA	AralarWT	2523 ± 260	2563 ± 237	1568 ± 221	1543 ± 133	1558 ± 68	1442 ± 103
	Aralar KO	1512 ± 141**	2682 ± 116	1223 ± 159	1979 ± 194*	1863 ± 88**	1062 ± 93
	(% vs WT)	60%	–	–	128%	119%	–

Results are expressed in nmol per g of tissue. Values are the mean ± SEM (n = 3–6). Statistical analysis was performed by one-way analysis of variance followed by Student-Newman-Keuls t-test.

*$p < 0.05$ Aralar-KO versus Aralar-WT mice.

**$p < 0.01$ Aralar-KO versus Aralar-WT mice.

***$p < 0.001$ Aralar-KO versus Aralar-WT mice.

striatum and limbic system (Table 2), which have much lower 5HT content than the former areas. Of note, mRNA for serotonin transporter (SERT/Slc6a4), the plasma membrane transporter of serotonin which terminates the action of serotonin, is greatly increased (5.5-fold of WT value) in Aralar-KO brain (Table S3), suggesting an increased reuptake of this neurotransmitter in brain from Aralar-KO mice.

In the brainstem, where the DAergic neuronal somata of the nigrostriatal pathway are located, no obvious change in the number of TH-positive cells was apparent (Fig. 3d). Neither the substantia nigra nor the midbrain from Aralar-KO mice showed changes in TH-immunolabeling (Fig. 3c) or expression of TH (not shown) as compared with WT. Moreover, DA and its metabolites were increased or unchanged in brainstem and diencephalon, the major regions enriched in DAergic somata, from Aralar-KO mice (Table 2).

In contrast, Aralar deficiency resulted in changes in DA and its metabolites in the regions enriched in DAergic projections, striatum, and limbic system. Aralar-KO striatum showed a substantial reduction in DA (to 64%) and its metabolites, 3-MT (to 43%) and HVA (to 68% of controls) (Table 2). However, the content of DOPAC was not changed, resulting in a significant increase in DOPAC/DA ratio (138% vs. control, Fig. 4a). The very low levels of 3-MT (Wood and Altar 1988; Brown *et al.* 1991) in striatum from Aralar-deficient mice and the increase in the ratio of the MAO-derived DA metabolite, DOPAC, over the catechol-*ortho*-methyl-transferase (COMT)-derived DA metabolites, 3-MT and HVA, in Aralar-KO striatum (DOPAC/HVA, 1.38-fold of WT (Fig. 4a); and DOPAC/3-MT, 2.35-fold of WT (data not shown)) suggest an impairment in DA release in these animals. As DOPAC formation requires the intraneuronal MAO–aldehyde dehydrogenase pathway, these results also suggests an increase in intraneuronal metabolism of DA in Aralar-KO mice (see Fig. 4c).

Aralar-KO limbic system shows an important reduction in DA (57%) and DOPAC (50%); but only a slight non-significant decrease in HVA (Table 2). Given that DOPAC/DA ratio was unchanged, the drop in DA content in the limbic system of Aralar-KO mice does not appear to be because of increased intracellular metabolism of DA (Fig 4a).

In conclusion, the Aralar-KO mouse brain shows no changes in NA but a significant decrease in 5-HT only in diencephalon and brainstem, brain regions rich in 5-HT neurons. As for the DA system, although DA and metabolites did not change in brain regions rich in DA somata, that is, diencephalon and brainstem, marked decreases in DA were found in areas enriched in DAergic nerve terminals. These results (Fig. 4a) suggest a clear increase in intraneuronal DA metabolism in striatum, but no obvious changes in the limbic system.

Table 2 Monoamine metabolism in striatum, diencephalon, limbic system, and brainstem of Aralar-WT mice and Aralar-KO mice

Monoamines (ng/g tissue)		Striatum	Diencephalon	Limbic system	Brain stem
DA	AralarWT	5690 ± 525	341 ± 92	1412 ± 220	97.7 ± 18
	Aralar KO	3661 ± 175**	431 ± 88	810 ± 82*	164 ± 51
	(% vs. WT)	64%	–	57%	–
3-MT	AralarWT	330 ± 39	n.d ≤ 6	59.7 ± 6.2	n.d ≤ 6
	Aralar KO	142 ± 29**	n.d ≤ 6	n.d ≤ 6	n.d ≤ 6
	(% vs. WT)	43%	–	–	–
DOPAC	Aralar WT	387 ± 10	84 ± 10	141 ± 14	43.8 ± 2.7
	Aralar KO	362 ± 38	127 ± 10*	71 ± 17**	73.7 ± 8**
	(% vs. WT)	–	151%	50%	168%
HVA	Aralar WT	681 ± 35	219 ± 21	136.5 ± 12.1	61.6 ± 6.4
	Aralar KO	468 ± 64*	279 ± 18	115.2 ± 6.6	85.2 ± 7.5*
	(% vs. WT)	68%	–	–	138 ± 12.2%
NA	Aralar WT	251 ± 20	846 ± 22	336 ± 20	1223 ± 60
	Aralar KO	265 ± 30	1008 ± 98	320 ± 28.8	1359 ± 36.5
	(% vs. WT)	–	–	–	–
5-HT	Aralar WT	333 ± 67	1501 ± 242	585 ± 55	1988 ± 39
	Aralar KO	250 ± 89	768 ± 88*	460 ± 58	1445 ± 172*
	(% vs. WT)	–	51%	–	72%
5-HIAA	Aralar WT	256 ± 102	859 ± 95	337 ± 40	484 ± 16
	Aralar KO	99 ± 28	375 ± 42***	218 ± 29.5*	285 ± 25***
	(% vs. WT)	–	43%	64%	59%

Results are expresssed in ng per g of tissue. Values are the mean ± SEM ($n = 6$). Statistical analysis was performed by one-way analysis of variance followed by Student-Newman-Keuls *t*-test.

*$p < 0.05$ Aralar-KO mice versus Aralar-WT mice.

**$p < 0.01$ Aralar-KO mice versus Aralar-WT mice.

***$p < 0.001$ Aralar-KO mice versus Aralar-WT mice.

DA markers of presynaptic and post-synaptic terminals in striatum and limbic system from Aralar-KO mice

A further analysis for DA markers in striatum and limbic system is shown in Fig. 4d–f. Remarkably, there is a significant reduction of the DAergic markers VMAT2, the presynaptic vesicular transporter of monoamines, and DARPP32, the dopamine and cAMP regulated phosphoprotein of 32 kDa present in striatal post-synaptic medium spiny neurons (Fienberg *et al.* 1998) in striatum (Fig. 4e), but not in the limbic system (Fig. 4f) of Aralar-KO mice. However, no changes in TH and the dopamine transporter DAT were found in striatum from Aralar-KO mice indicating no gross modifications in the density of presynaptic DAergic terminals (Fig. 4d). The content of GFAP and OX6 as gliosis markers was unchanged in Aralar-deficient striatum compared with controls (not shown).

DARPP32 is mainly expressed in mature medium spiny neurons which are GABAergic (Fienberg *et al.* 1998). We have previously noted a 40% decrease in striatal GABA levels in Aralar-KO mice (Table 1). However, the remarkable lack of post-synaptic DARPP32 in striatum from Aralar-deficient mice (Fig. 4e) was not accompanied by any change in the GABA synthesis enzyme GAD65, a more immature marker for GABA-containing neurons (not shown). These results suggest a deficiency in maturation of medium spiny GABA neurons in Aralar-deficient striatum.

Regarding presynaptic DA terminals, the fall in VMAT2 (of about 42%) suggests that the vesicular storage of DA is also impaired in Aralar-deficient striatum.

Increased oxidative stress in Aralar-KO striatum

The increase in the DOPAC/DA ratio in Aralar-KO striatum (Fig. 4a) indicates an increased intracellular oxidation of DA which would lead to an increase of H_2O_2 formation via mitochondrial MAO activity (Fig. 5) which could result in a selective oxidative stress in DAergic neurons (Spina and Cohen 1989). To verify this hypothesis, we measured the content of reduced (GSH) and oxidized glutathione (GSSG) in striatum and other brain regions (limbic system and brainstem) as readout of the cellular redox state (White *et al.* 1986; Spina and Cohen 1989).

No changes in GSH levels were found in striatum but the content of GSSG was more than two-fold higher in Aralar-KO compared to WT mice (Fig. 4b). GSH and GSSG content in Aralar-KO mice was unchanged in the other brain regions analyzed (limbic system and brainstem; Figure S2).

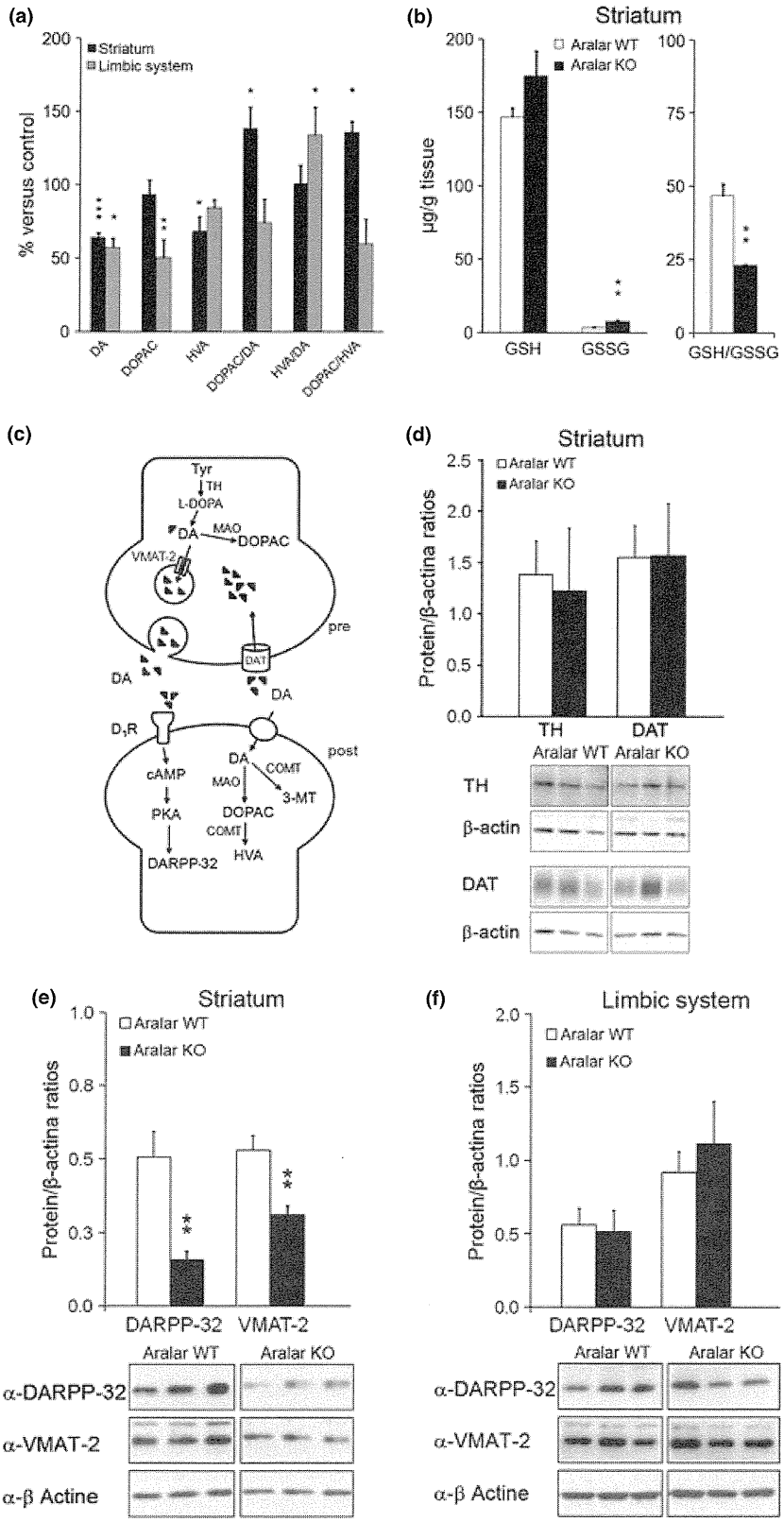

Fig. 4 Striatum appeared to be the most affected region in Aralar-knock-out (KO) brain. (a) Differential effects of Aralar deficiency on dopamine (DA) metabolism in brain regions enriched in DA terminals (striatum and limbic system). DA and its metabolites, except 3,4 dihydroxy-phenyl acetic acid (DOPAC), are significantly decreased in Aralar-KO striatum. DA turnover is increased in Aralar-KO striatum. (b) The enhanced striatal DA turnover provoked an increase in cellular oxidative stress as measured by GSH/GSSG ratios. (c) Scheme of tyrosine metabolism into the presynaptic and post-synaptic neurons in striatum, representing metabolites, enzymes, and proteins involved. (d–f) Expression of dopamine markers in Aralar-KO striatum and limbic system. Representative western blot of tyrosine hydroxylase (TH), dopamine transporter (DAT) in striatum (d); and vesicular monoamine transporter 2 (VMAT2), dopamine and cAMP regulated phosphoprotein of 32 KDa (DARPP32) proteins in striatum (e) and limbic system (f) with their respective densitometric histograms. β-actin was used as charge control. Results are expressed as the mean ± SEM ($n = 6$ mice per group). Statistical analysis was performed by one-way ANOVA followed by Newman–Keuls test. $^{*}p \leq 0.05$, $^{**}p \leq 0.01$, $^{***}p \leq 0.001$.

The decreased GSH/GSSG ratio in Aralar-deficient striatum suggests that this brain region is subjected to high oxidative stress (Figs 4b and 5).

Aralar-hemizygous adult mice also show increased intraneuronal dopamine metabolism

The affectation observed in striatum from Aralar-KO mice (PND20) prompted us to analyze monoamine metabolism in striatum of adult and healthy mice expressing only half-a-dose of Aralar (Fig. 6). Mice expressing 50% normal Aralar/AGC1 (hemizygous) are indistinguishable from wild-type siblings and thrive and survive normally (not shown). In striatum, DA and 5-HT content was not altered by half-a-dose of Aralar expression versus control (Fig. 6a), but DOPAC content was significantly increased. Hemizygous-Aralar (HT) adult mice display an increased metabolism of DA by MAO (DOPAC/DA ratio was 135% higher in striatum of Aralar-HT vs. Aralar-WT mice at 18 months of age), ($p = 0.0055$, $n = 7$; Fig. 6a).

Hemizygous-Aralar mice presented also an enhanced sensitivity to the locomotor stimulating effects of amphetamine (Fig. 6c–f). Amphetamine provoked a dose-dependent increase in average speed in both genotypes, with a more pronounced effect in HT mice (Fig. 6c), reaching a plateau at 5.0 mg/kg. At 3.0 mg/kg dose of intraperitoneal

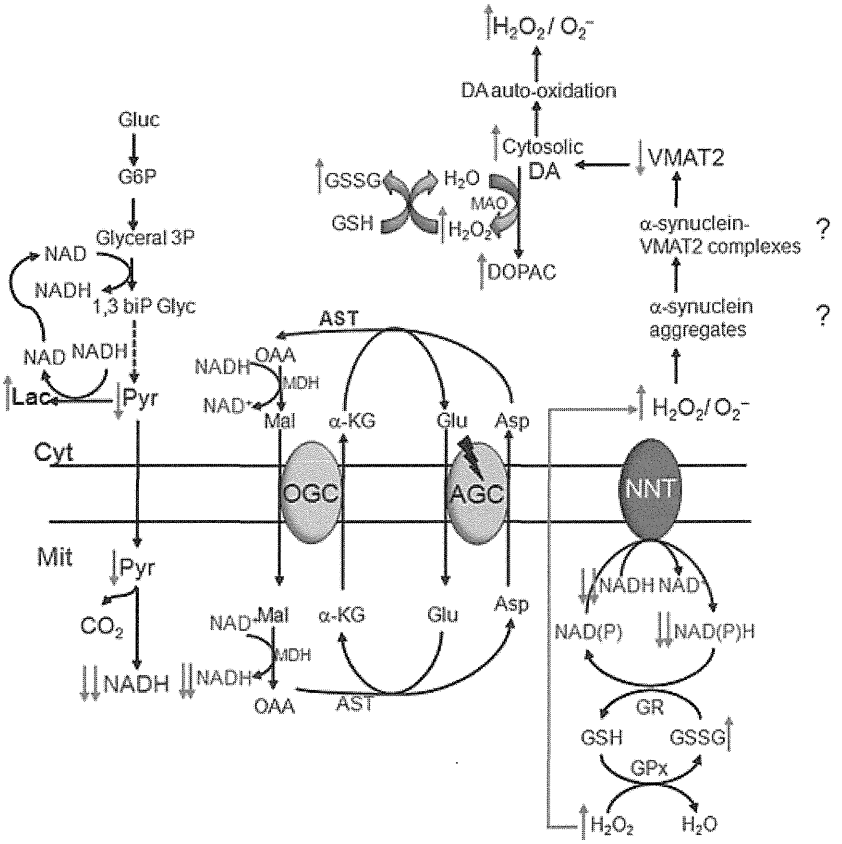

Fig. 5 Mechanism for toxicity induced by the lack of Aralar in DAergic nigrostriatal nerve terminals. Lack of Aralar-MAS activity causes a decrease in mitochondrial NADH because both lack of redox transfer by the shuttle and limited pyruvate supply to mitochondria; and also decreased mitochondrial NAD(P)H content. As glutathione system (and thioredoxin) for ROS detoxification is reduced by the mitochondrial NADPH pool, increased ROS is expected to happen in Aralar-deficient mitochondria. Mitochondrial ROS (O_2^- and H_2O_2) diffuse to the cytosol, presumably provoking increased levels of cytosolic alpha-synuclein aggregates and synuclein-VMAT2 complexes in the presynaptic DA nerve terminals of Aralar-knock-out (KO) mice, with loss of VMAT2. Consequently, an increase in non-vascularized cytosolic DA produces an enhancement in DA autoxidation and in enzymatic oxidation via MAO activity (with higher DOPAC/DA ratio). Both pathways involve an overproduction of ROS, as reflected by increased GSSG, in Aralar-KO striatum. This further potentiates VMAT2 decline and possibly loss of function in the DA terminal with the subsequent mishandling of DA. AGC, aspartate-glutamate carrier; Asp, aspartate; AAT, aspartate aminotransferase; DA, dopamine; DOPAC, 3,4-dihydroxy-phenylacetic acid; G6P, glucose 6 phosphate; Glu, glutamate; Gluc, glucose; GA3P, glyceraldehyde 3-phosphate; GPx, glutathione peroxidase; GR, glutathione reductase; GSH, reduced glutathione; GSSG, oxidized glutathione; α-KG; α-ketoglutarate; Lac, lactate; Mal, malate; MAO, monoamine oxidase; MDH, malate dehydrogenase; NNT, NADH-NADP-transhydrogenase; OAA, oxalacetic acid; OGC, α-ketoglutarate-malate carrier; Pyr, pyruvate; VMAT2, vesicular monoamine transporter 2.

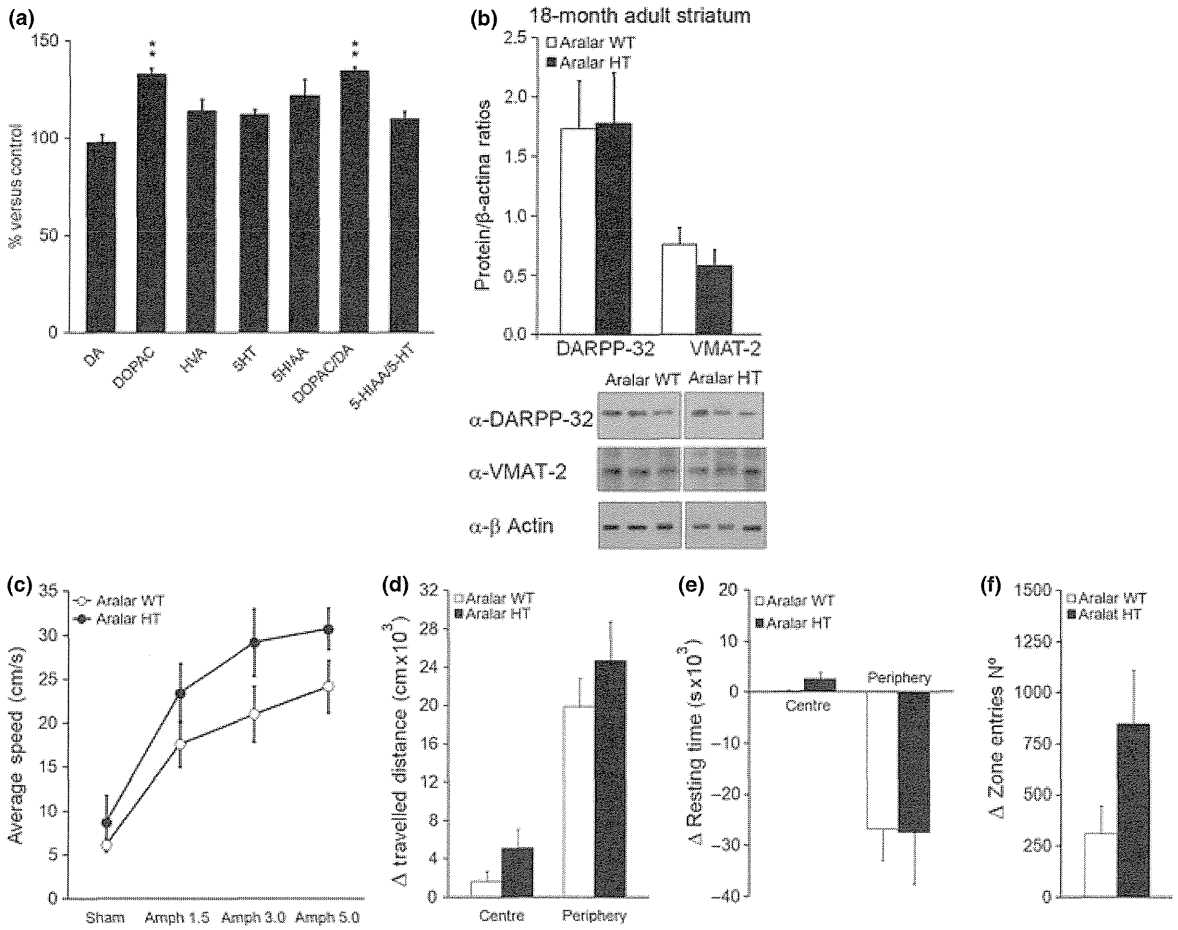

Fig. 6 Alteration of striatal dopamine handling in adult and healthy Aralar-hemizygous mice at 18-months old. (a) Cytosolic dopamine (DA) metabolism is significantly increased in Aralar-HM striatum as compared with wild-type mice, without changes in the content of monoamines between genotypes. Values (ng/g tissue) in control striatum are as follows: DA, 14583 ± 258; 3,4 dihydroxy-phenyl acetic acid (DOPAC), 782 ± 21; homovanillic acid (HVA), 923 ± 24; serotonin (5-HT), 1252 ± 36; 5-HIAA, 291 ± 13. ($n = 7$). (b) Representative western blot of vesicular monoamine transporter 2 (VMAT2), dopamine and cAMP regulated phosphoprotein of 32 KDa (DARPP32) proteins in striatum with their respective densitometric histograms. β-actin was used as charge control. ($n = 6$). (c–f) Increased sensitivity to the motor effects of systemic amphetamine in Aralar-HM mice. Open field parameters as average speed (c), traveled distance (d), resting time between displacements (e), and the number of zone entries (f) in the center and periphery of the arena are valutated in WT and Aralar-hemizygote mice. Results are expressed as the mean ± SEM ($n = 7$). Statistical analysis was performed by one-way ANOVA followed by Newman–Keuls test. $^{**}p \leq 0.01$.

amphetamine, a higher increment in traveled distance (Fig 6d), with the consequent decrease in resting time (Fig. 6e), in relation to that observed at sham administration was found in HT as compared with WT. A similar course is observed in the number of entries in center and periphery (Fig. 6f). VMAT2 was only slightly decreased to 73% in striatum of Aralar-HT adult mice as compared with control littermates (Fig. 6b). However, a higher decrease in VMAT2 content was found in striatum from Aralar-KO mice (Fig. 4e). As amphetamine is thought to release newly formed, mostly cytoplasmic rather than vesicular, catecholamines (Itier *et al.* 2003), these findings suggest that the reduction of Aralar-MAS activity alter the handling of intracytoplasmic neurotransmitters as DA.

Discussion

Aralar-KO mice present a short lifespan, dying at PND22–23, with generalized tremor, severe hypomyelination (Jalil *et al.* 2005) and modifications in cortical projections but with no apparent neuronal cell death (Sakurai *et al.* 2010; Ramos *et al.* 2011). Herein, we show that Aralar-KO mice exhibit a higher exploratory activity, hyperactivity, hyperreactivity, and anxious-like behavior with aversive conditions as well as an increase in rearing; parameters that are known to be sensitive to interferences with the DAergic system (Bernardi *et al.* 1981). In addition, Aralar-KO mice have a loss in motor coordination and alterations in the gait pattern and equilibrium, deficits that have been extensively associated to

striatal DAergic damage (Menéndez *et al.* 2006; Taylor *et al.* 2011). Failure to perform homing test, in Aralar-KO mice, constitutes a reliable indicator of reduced motivation associated to dopamine deficiency (Palmiter 2008). According to the behavior observations, KO mice (PND20) showed depletion of DA in DA projection-rich areas, striatum, and limbic system, where levels of DA and its metabolites are highest [60-fold higher DA in striatum than brainstem (Table 2)]; and DA mishandling was reflected by significant increased DOPAC/DA ratio in Aralar-KO striatum. DA mishandling was also found in striatum of adult (18-months old) and healthy Aralar-hemizygote mice (Fig. 6). The KO mice also showed a marked decrease in 5-HT and its metabolite 5-HIAA in brainstem and diencephalon, the regions with higher 5-HT levels in control animals. An increase in locomotion and DA metabolism could be associated to acceleration of cellular DA uptake (Husain *et al.* 1994), as supported by the higher DAT/VMAT2 ratio found in Aralar-KO striatum as compared with controls. However, hyperactivity in open field might be also related to anxiety-dependent behavior, because of DA (Zweifel *et al.* 2011) and 5HT depletions (for review, Fernandez and Gaspar 2011), as it was only detected in novelty-related experimental situations.

Our results indicate that the nigrostriatal DAergic system and striatum are preferentially vulnerable to Aralar-MAS deficiency associated to DA mishandling; and previously, we showed that the lack of Aralar-MAS induces a decrease in the maximal respiratory capacity in neurons (Gómez-Galán *et al.* 2011). These observations are well in agreement with the notion that striatum is highly susceptible to mitochondrial metabolic dysfunctions (Zeevalk *et al.* 1997; Watabe and Nakaki 2008; Pickrell *et al.* 2011; Sterky *et al.* 2012). Together with these findings, fall in striatal GABA and a pronounced decline in glutamate and glutamine were found. Our results now reveal two new defects related to Aralar deficiency in striatum: (i) Inability of GABAergic striatal neurons to achieve a mature phenotype. These neurons remain immature as reflected by the spared DARPP32 (a protein that mediates DAergic neurotransmission in almost all the medium spiny neurons), with little variations in GABA or GAD65 expression (Lauder *et al.* 1986); and (ii) loss of DA and DA mishandling reflected by increased DOPAC/DA ratio. The significant reduction in striatal VMAT2 of Aralar-KO mice supports that the presynaptic DAergic nerve endings are damaged but still present as DAergic markers as TH and DAT were unaffected. In contrast to striatum, in regions enriched in DAergic somata as brainstem and diencephalon, DA content was found to be increased, perhaps because of an attempt to compensate for any dysfunction in the surviving DAergic neurons, as occurs in the very early stages of Parkinson's disease (PD) (Hefti *et al.* 1980; Altar *et al.* 1987; Hornykiewicz and Kish 1987).

The impairment of the dopaminergic system, particularly in the dopaminergic striatal terminals of the Aralar-KO mouse, is probably related to an increase in oxidative stress caused by the lack of Aralar-MAS activity which adds to the known vulnerability of these terminals to oxidative stress. This increased oxidative stress was reflected, in the very significant decrease in the GSH/GSSG ratio specifically in Aralar-KO striatum. The decrease in GSH/GSSG in Aralar-KO striatum most likely reflects an increased oxidative stress in the cytosol which has the largest GSH pool and/or the mitochondria that contains a much smaller GSH pool (Spina and Cohen 1989; Murphy 2012). Although we believe that the initial decrease in GSH is mitochondrial (see below), H_2O_2 escaped from mitochondria to the cytosol probably contributes to the decrease in cytosolic GSH/GSSG.

Mitochondria produce O_2^- and H_2O_2 which are detoxified due to GSH and thioredoxin together with a number of enzymes that ultimately use one of these two thiol molecules as redox agents (Murphy 2012). The regeneration of the reduced forms of glutathione and thioredoxin requires NADPH. There are three systems which produce NADPH in brain mitochondria, NADP-isocitrate dehydrogenase, malic enzyme, and energy dependent nicotinamide nucleotide transhydrogenase (NNT) (Andres *et al.* 1980; Albracht *et al.* 2011). The third of these systems, NNT, utilizes mitochondrial NADH and the proton electrochemical gradient to produce NADPH. There is evidence that NNT is important in supplying NADPH for mitochondrial detoxification, as the lack of NNT increased O_2^-/H_2O_2 production in mitochondria of beta cells (Freeman *et al.* 2006), and impairs cellular redox homeostasis and energy metabolism in human adrenocortical (Meimaridou *et al.* 2012) and pheochromocytoma cells (Yin *et al.* 2012).

NADPH production through NNT may be limited by mitochondrial NADH production. In brain, which utilizes glucose as main energy source, mitochondria produce NADH from pyruvate in the tricarboxylic acid cycle. The lack of Aralar results in a pronounced decrease in MAS, the major NADH shuttle in brain (Jalil *et al.* 2005), resulting in an increased lactate-to-pyruvate ratio (Pardo *et al.* 2011), and in a limitation in pyruvate supply to mitochondria as reflected in a reduced maximal respiration rate in intact neurons (Gómez-Galán *et al.* 2011). This scenario is one in which mitochondrial NADH production is clearly limited, and this will result in a lack of inactivation of O_2^- and H_2O_2 which will cause oxidative damage to Aralar-KO mitochondria, and the escape of H_2O_2 to the cytosol (Han *et al.* 2003), causing oxidative stress in this cellular compartment.

ROS formation is further potentiated in Aralar-KO striatum because VMAT2 deficiency resulting in an increase in non-vesicular DA that might favor both MAO-mediated oxidation and autooxidation of non-protected cytosolic DA. These two processes lead to the formation of ROS, such as hydrogen peroxide, and reactive quinone and semi-quinone

species produced by DA autooxidation (Graham 1978; Maker *et al.* 1981). Furthermore, DACHR (*o*-quinone dopaminochrome, a product of DA oxidation) has been reported to increase, in a dose-dependent way, the production of H_2O_2 constitutively observed at Complex I of the mitochondrial respiratory chain (Zoccarato *et al.* 2005). Our data suggest that the rate of production of ROS evoked by Aralar deficiency in striatum override cellular mechanisms for reducing GSSG and might have important consequences in DA neuronal physiology, which is particularly sensitive to oxidative stress (Zeevalk *et al.* 1997; Drechsel and Patel 2008).

Decreased VMAT2 expression was found exclusively in striatum, but not in limbic system, of Aralar-KO mice. A similar finding was reported as a key pathogenic event preceding nigrostriatal dopamine neurodegeneration and clinical manifestations in a primate model of PD and attributed to an association of VMAT2 with α-synuclein aggregates induced by oxidative stress as a result of (1-methyl-4-phenyl-1,2,3,6-tetrahydropiridine) MPTP treatment (Chen *et al.* 2008a). A direct interaction between VMAT2 and α-synuclein with disruption of synaptic vesicle dynamics has been proposed by other groups (Lotharius and Brundin 2002; Mosharov *et al.* 2006; Guo *et al.* 2008; for references, Taylor *et al.* 2011). The loss of VMAT2 in the Aralar-KO mice might be also because of sequestration with α-synuclein aggregates but this remains an open question. The mishandling of DA via reduced VMAT2, associated to an increased striatal DOPAC/DA (Fig. 4a), and GSSG/GSH ratios (Fig. 4b), might be sufficient to cause DA-mediated toxicity and neurodegeneration in the nigrostriatal DA system (Mooslehner *et al.* 2001; Caudle *et al.* 2007; Chen *et al.* 2008b; for review, see Taylor *et al.* 2011). The specific vulnerability of nigrostriatal DA neurons might be explained because they have a higher ROS formation than those DA neurons in limbic system (Surmeier *et al.* 2011) and also these A9 DA neurons are specially prone to ROS attack, that is, the scarce proportion of glial cells surrounding DA neurons in the substantia nigra (for review, Mena *et al.* 2002), the presence of neuromelanin pigment in subpopulations of DA-containing mesencephalic neurons (Hirsch *et al.* 1988) and the low content of mitochondria in DA neurons of the substantia nigra pars compacta (Liang *et al.* 2007) might be mentioned between other characteristics.

The results demonstrate that AGC1-MAS deficiency in mice targets monoaminergic brain systems in striatum. DA neurotransmission is also altered in mice with mutations of α-synuclein, parkin or DJ-1, considered suitable models for PD studies. These mice, as reported herein for Aralar-KO and previously for VMAT2-KO mice (Colebrooke *et al.* 2006), do not display loss of midbrain DA neurons, the hallmark of Parkinson's disease (Dawson *et al.* 2010; for references). Perhaps, DA neurons do not degenerate in the mouse models because there are compensatory mechanisms that prevent the loss of DA neurons during their short lifespan. Also, it is worth to take into account that mice possess low neuromelanin and high GSH content what might render them specially resistant to DA degeneration compared with primates and humans (Hirsch *et al.* 1988; Itier *et al.* 2003, for references). These factors would contribute to underestimate the putative detrimental effects of Aralar-MAS deficiency on the DA system in humans. Deficiencies or failure in the operation of the Aralar-MAS pathway, resulting in a limited mitochondrial NADH formation, NNT function and ROS detoxifying capacity, might constitute an important factor at the origin of DA degeneration and its implication in human pathologies as Parkinson's and Huntington's diseases might be thoughtfully explored.

Acknowledgements

This study was supported by grants from the Ministerio de Educación y Ciencia BFU2008-04084/BMC (to JS), and Ciencia e Innovación (SAF2010-16427 to MD), Comunidad de Madrid S-GEN-0269-2006 MITOLAB-CM (to JS), European Union Grant LSHM-CT-2006-518153 (to J.S.), and CureFXS E-Rare. EU/FIS PS09102673, Spanish Ministry of Health (PI 082038 to MD), Marató TV3, Jerome Lejeune (JMLM/AC/08-044) to MD, Fundación Médica Mutua Madrileña (to BP), and by an institutional grant from the Fundación Ramón Areces to the CBMSO. CIBERER is an initiative of the ISCIII.

The authors thank to Isabel Manso, Barbara Sesé and Dolores Cano for technical support. IL-F is a recipient of a predoctoral contract from the Comunidad de Madrid, Spain.

Conflict of interest

None declared.

Supporting information

Additional supporting information may be found in the online version of this article at the publisher's web-site.

Figure S1. (a–b) Representative images of muscle sections obtained from gastronemius of Aralar-KO and WT mice at 20 PND stained with TCR (a) and NADH-TR (b).

Figure S2. The content of GSH and GSSG was not significantly different in limbic sytem (a) and brainstem (b).

Table S1. Enzymes with a significant 2-fold increase or reduction in the Aralar-KO mouse.

Table S2. Demyelination-related genes.

Table S3. Aminoacid and metabolite transport.

References

Albracht S. P., Meijer A. J. and Rydström J. (2011) Mammalian NADH: ubiquinone oxidoreductase (Complex I) and nicotinamide nucleotide transhydrogenase (Nnt) together regulate the mitochondrial production of H_2O_2-Implications for their role in disease, especially cancer. *J. Bioenerg. Biomembr.* **43**, 541–564.

Altar C. A., Marien M. R. and Marshall J. F. (1987) Time course of adaptations in dopamine biosynthesis, metabolism, and release following nigrostriatal lesions: implications for behavioral recovery from brain injury. *J. Neurochem.* **48**, 390–399.

Andres A., Satrústegui J. and Machado A. (1980) Development of NADPH producing pathways in rat heart. *Biochem. J.* **186**, 799–803.

Berkich D. A., Ola M. S., Cole J., Sweatt A. J., Hutson S. M. and LaNoue K. F. (2007) Mitochondrial transport proteins of the brain. *J. Neurosci. Res.* **85**, 3367–3377.

Bernardi M. M., De Souza H. and Palermo Neto J. (1981) Effects of single and long-term haloperidol administration on open field behavior of rats. *Psychopharmacology* **73**, 171–175.

Brown E. E., Damsma G., Cumming P. and Fibiger H. C. (1991) Intersticial 3-methoxytyramine reflects striatal dopamine release: an in vivo microdialysis study. *J. Neurochem.* **57**, 701–707.

Cahoy J. D., Emery B., Kaushal A. *et al.* (2008) A transcriptome database for astrocytes, neurons, and oligodendrocytes: a new resource for understanding brain development and function. *J. Neurosci.* **28**, 264–278.

Canals S., Casarejos M. J., Rodriguez-Martin E., de Bernardo S. and Mena M. A. (2001) Neurotrophic and neurotoxic effects of nitric oxide on fetal midbrain cultures. *J. Neurochem.* **76**, 56–68.

Carlsson A. and Lindqvist M. (1973) Effect of ethanol on the hydroxylation of tyrosine and tryptophan in rat brain in vivo. *J. Pharm. Pharmacol.* **25**, 437–440.

Carola V., DÓlimpio F., Brunamonti E., Mangia F. and Renzi P. (2002) Evaluation of the elevated plus-maze and open-field tests for the assessment of anxiety-related behavior in inbred mice. *Behav. Brain Res.* **144**, 49–57.

Caudle W. M., Richardson J. R., Shepherd K. R., Taylor T. N., Guillot T. S., McCormack A. L., Colebrooke R. E., Di Monte D. A., Emson P. C. and Miller G. W. (2007) Reduced vesicular storage of dopamine causes progressive nigrostriatal neurodegeneration. *J. Neurosci.* **27**, 8138–8148.

Chen M. K., Kuwabara H., Zhou Y. *et al.* (2008a) VMAT2 and dopamine neuron loss in a primate model of Parkinson's disease. *J. Neurochem.* **105**, 78–90.

Chen L., Ding Y., Cagniard B., Van Laar A. D., Mortimer A., Chi W., Hastings T. G. and kang U.J., and Zhuang X. (2008b) Unregulated cytosolic dopamine causes neurodegeneration associated with oxidative stress in mice. *J. Neurosci.* **28**, 425–433.

Colebrooke R. E., Humby T., Lynch P. J., McGowan D. P., Xia J. and Emson P. C. (2006) Age-related decline in striatal dopamine content and motor performance occurs in the absence of nigral cell loss in a genetic mouse model of Parkinson's disease. *Eur. J. Neurosci.* **24**, 2622–2630.

Contreras L., Urbieta A., Kobayashi K., Saheki T. and Satrústegui J. (2010) Low levels of citrin (SLC25A13) expression in adult mouse brain restricted to neuronal clusters. *J. Neurosci. Res.* **88**, 1009–1016.

Dawson T. M., Ko H. S. and Dawson V. L. (2010) Genetic animal models of Parkinson's disease. *Neuron* **66**, 646–661.

Del Arco A. and Satrústegui J. (1998) Molecular cloning of aralar, a new member of the mitochodrial carrier superfamily that binds calcium and is present in human muscle and brain. *J. Biol. Chem.* **273**, 23327–23334.

Drechsel D. A. and Patel M. (2008) Role of reactive oxygen species in the neurotoxicity of environmental agents implicated in Parlkinson' s disease. *Free Radic. Biol. Med.* **44**, 1873–1886.

Fernandez S. P. and Gaspar P. (2011) Investigating anxiety and depressive-like phenotypes in genetic mouse models of serotonin depletion. *Neuropharmacology* **62**, 144–154.

Fienberg A. A., Hiroi N., Mermelstein P. G. *et al.* (1998) DARPP-32: Regulator of the efficacy of dopaminergic neurotransmission. *Science* **281**, 838–842.

Freeman H., Shimomura K., Horner E., Cox R. D. and Ashcroft F. M. (2006) Nicotinamide nucleotide transhydrogenase: a key role in insulin secretion. *Cell Metab.* **3**, 35–45.

Gómez-Galán M., Makarova J., Llorente-Folch I., Saheki T., Pardo B., Satrústegui J. and Herreras O. (2011) Altered postnatal development of cortico-hippocampal neuronal electric activity in mice deficient for the mitochondrial aspartate-glutamate transporter. *J. Cereb. Blood Flow Metab.* **32**, 306–317.

Graham D. G. (1978) Oxidative pathways for catecholamines in the genesis of neuromelanin and cytotoxic quinones. *Mol. Pharmacol.* **14**, 633–643.

Griffith O.W. (1980) Determination of glutathione and glutathione disulfide using glutathione reductase and 2-vinylpyridine. *Anal. Biochem.* **106**, 207–212.

Guo J. T., Chen A. N. Q., Kong Q. I., Zhu H., Ma C. M. and Qin C. (2008) Inhibition of vesicular monoamine transporter-2 activity in -synuclein stably transfected SH-SY5Y cells. *Cell. Mol. Neurobiol.* **28**, 35–47.

Han D., Antunes F., Canali R., Rettori D. and Cadenas E. (2003) Voltage-dependent anion channels control the release of the superoxide anion from mitochondria to cytosol. *J. Biol. Chem.* **278**, 5557–5563.

Hauber W. (1998) Involvement of basal ganglia transmitter system in movement initiation. *Prog. Neurobiol.* **56**, 507–540.

Hefti F., Melamed E. and Wurtman R. J. (1980) Partial lesions of the dopaminergic nigrostriatal system in rat brain: biochemical characterization. *Brain Res.* **195**, 123–137.

Hirsch E., Graybiel A. M. and Agid Y. A. (1988) Melanized dopaminergic neurons are diferentially susceptible to degeneration in Parkinson's disease. *Nature* **334**, 345–348.

Hornykiewicz O. and Kish S. J. (1987) Biochemical pathophysiology of Parkinson's disease. *Adv. Neurol.* **45**, 19–34.

Husain R., Malaviya M., Seth P. K. and Husain R. (1994) Effect of deltamethrin on regional brain polyamines and behaviour in young rats. *Pharmacol. Toxicol.* **74**, 211–215.

Itier J.-M., Ibañez P., Mena M. A. *et al.* (2003) Parkin gene inactivation alters behaviour and dopamine neurotransmission in the mouse. *Hum. Mol. Genet.* **12**, 2277–2291.

Jalil M. A., Begum L., Contreras L. *et al.* (2005) Reduced N-acetylaspartate levels in mice lacking Aralar, a brain- and muscle-type mitochondrial aspartate-glutamate carrier" *J. Biol. Chem.* **280**, 31333–31339.

Lauder J. M., Han V. K., Henserson P., Verdoon T. and Towle A. C. (1986) Prenatal ontogeny of the GABAergic system in the rat brain: an immunocytochemical study. *Neuroscience* **19**, 465–493.

Liang C. L., Wang T. T., Luby-Phelps K. and German D. C. (2007) Mitochondria mass is low in mouse substantia nigra dopamine neurons: implications for Parkinson's disease. *Exp. Neurol.* **203**, 370–380.

Liu M., Liu H. and Dudley S. C. Jr (2010) Reactive oxygen species originating from mitocondria regulate the cardiac sodium cannel. *Circ. Res.* **107**, 967–974.

Lotharius J. and Brundin P. (2002) Pathogenesis of Parkinson's disease: dopamine, vesicles and alpha-synuclein. *Nat. Rev. Neurosci.* **3**, 932–942.

Maker H. S., Weiss C., Silides D. J. and Cohen G. (1981) Couple of dopamine oxidation monoamine oxidation via the generation of hydrogen peroxide in rat brain homogenates. *J. Neurochem.* **36**, 589–593.

Martínez de Lagrán M., Altafaj X., Gallego X., Martí E., Estivill X., Sahún I., Fillat C. and Dierssen M. (2004) Motor phenotypic alterations in TgDyrK1a transgenic mice implicate DYRK1A in Down syndrome motor dysfunction. *Neurobiol. Disease* **15**, 132–142.

Meimaridou E., Kowalczyk J., Guasti L. *et al.* (2012) Mutations in *NNT* encoding nicotinamide nucleotide transhydrogenase cause familial glucocorticoid deficiency. *Nat. Genet.* **44**, 740–742.

Mena M. A., Pardo B., Paino C. L. and De Yébenes J. G. (1993) Levodopa toxicity in foetal rat midbrain neurones in culture: modulation by ascorbic acid. *NeuroReport* **4**, 438–440.

Mena M. A., Garcia de Yébenes M. J., Tabernero C., Casarejos M. J., Pardo B. and Garcia de Yébenes J. (1995) Effects of calcium antagonists on the dopamine system. *Clin. Neuropharmacol.* **18**, 410–426.

Mena M. A., Khan U., Togasaki D. M., Sulzer D., Epstein C. J. and Przedborski S. (1997) Effects of wild-type and mutated copper/zinc superoxide dismutase on neuronal survival and L-DOPA-induced toxicity in postnatal midbrain culture. *J. Neurochem.* **69**, 21–33.

Mena M. A., de Bernardo S., Casarejos M. J., Canals S. and Rodríguez-Martin E. (2002) The role of astroglia on the survival of dopamine neurons. *Mol. Neurobiol.* **25**, 245–263.

Menéndez J., Rodríguez-Navarro J. A., Solano R. M., Casarejos M. J., Rodal I., Guerrero R., Sánchez M. P., Avila J., Mena M. A. and de Yébenes J. G. (2006) Supression of parkin enhances nigrostriatal and motor neuron lesion in mice over-expressing human-mutated tau protein. *Hum. Mol. Genet.* **15**, 2045–2058.

Mooslehner K. A., Chan P. M., Xu W., Liu L., Smadja C., Humby T., Allen N. D., Wilkinson L. S. and Emson P. C. (2001) Mice with very low expression of the vesicular monoamine transporter 2 gene survive into adulthood: potential mouse model for parkinsonism. *Mol. Cell. Biol.* **21**, 5321–5331.

Mosharov E. V., Staal R. G. W., Bové J. *et al.* (2006) -synuclein overexpression increases cytosolic catecholamine concentration. *J. Neurosci.* **26**, 9304–9311.

Murphy M. P. (2012) Mitochondrial thiols in antioxidant protection and redox signalling: distinct roles for glutathionylation and other thiol modifications. *Antioxid. Redox Signal.* **16**, 476–495.

Nguyen N. H., Brathe A. and Hassel B. (2003) Neuronal uptake and metabolism of glycerol and the neuronal expression of mitochondrial glycerol-3-phosphate dehydrogenase. *J. Neurochem.* **85**, 831–842.

Palmiter R. D. (2008) Dopamine signaling in the dorsal striatum is essential for motivated behaviors. Lessons for dopamine-deficient mice. *Ann. N. Y. Acad. Sci.* **1129**, 35–46.

Pardo B., Mena M. A., Casarejos M. J., Paino C. L. and de Yébenes J. G. (1995) Toxic effects of L-DOPA on mesencephalic cell cultures: protection with antioxidants. *Brain Res.* **682**, 133–143.

Pardo B., Contreras L., Serrano A., Ramos M., Kobayashi K., Iijima M., Saheki T. and Satrústegui J. (2006) Essential role of aralar in the transduction of small calcium signals to neuronal mitochondria. *J. Biol. Chem.* **281**, 1039–1047.

Pardo B., Rodrigues T. B., Contreras L., Garzón M., Llorente-Folch I., Kobayashi K., Saheki T., Cerdán S. and Satrústegui J. (2011) Brain glutamine synthesis requires neuronal-born aspartate as amino donor for glial glutamate formation. *J. Cereb. Blood Flow Metab.* **31**, 90–101.

Pickrell A. M., Fukui H., Wang X., Pinto M. and Moraes C. (2011) The striatum is highly susceptible to mitochondrial oxidative phosphorylation dysfunctions. *J. Neurosci.* **31**, 9895–9904.

Ramos M., del Arco A., Pardo B. *et al.* (2003) Developmental changes in the Ca^{2+} -regulated mitochondrial aspartate-glutamate carrier aralar1 in brain and prominent expression in the spinal cord. *Dev. Brain Res.* **143**, 33–46.

Ramos M., Pardo B., Llorente-Folch I., del Arco A. and Satrústegui J. (2011) The deficiency in the mitochondrial transporter of aspartate/glutamate Aralar/AGC1 causes hypomyelination and neuronal defects unrelated to myelin deficits in mouse brain. *J. Neurosci. Res.* **89**, 2008–2017.

Sakurai T., Ramoz N., Barreto M. *et al.* (2010) Slc25a12 disruption alters myelination and neurofilaments: a model for a hypomyelination syndrome and childhood neurodevelopmental disorders. *Biol. Psychiatry* **67**, 887–894.

Spina M. B. and Cohen G. (1989) Dopamine turnover and glutathione oxidation: implications for Parkinson's disease. *Proc. Natl Acad. Sci. USA* **88**, 1398–1400.

Stein J. M., Bergman W., Fang Y., Davison L., Brensinger C., Robinson M. B., Hecht N. B. and Abel T. (2006) Behavioral and neurochemical alterations in mice lacking tha RNA-binding protein translin. *J. Neurosci.* **26**, 2184–2196.

Sterky F. H., Hoffman A. F., Milenkovic D., Bao B., Paganelli A., Edgar D., Wibom R., Lupica C. R., Olson L. and Larsson N. G. (2012) Altered dopamine metabolism and increased vulnerability to MPTP in mice with partial deficiency of mitochondrial complex I in dopamine neurons. *Hum. Mol. Genet.* **21**, 1078–1089.

Surmeier D. J., Guzman J. N., Sanchez-Padilla J. and Schumacker P. T. (2011) The role of calcium and mitochondrial oxidant stress in the loss of substantia nigra pars compacta dopaminergic neurons in Parkinson's disease. *Neuroscience* **198**, 221–231.

Taylor T. N., Caudle W. M. and Miller G. W. (2011) VMAT2-deficient mice display nigral and extranigral pathology and motor and nonmotor symptoms of Parkinson's disease. *Parkinsons Dis.* 2011, 124165.

Tietze F. (1969) Enzymatic method for quantitative determination of nanogram amounts of total and oxidized glutathione: application to mammalian blood and other tissues. *Anal. Biochem.* **27**, 502–522.

Watabe M. and Nakaki T. (2008) Mitochondrial complex I inhibitor rotenone inhibits and redistributes vesicular monoamine transporter 2 via nitration in human dopaminergic SH-SY5Y cells. *Mol. Pharmacol.* **74**, 933–940.

White C. W., Mimmack R. F. and Repine J. E. (1986) Accumulation of lung tissue oxidized glutathione (GSSG) as a marker of oxidant induced lung injury. *Chest (Suppl.)* **89**, 111–113.

Wibom R., Lasorsa F. M., Töhönen V. *et al.* (2009) AGC1 deficiency associated with global cerebral hypomyelination. *N. Engl. J. Med.* **361**, 489–495.

Wood P. L. and Altar C. A. (1988) Dopamine release in vivo from nigrostriatal, mesolimbic and mesocortical neurons: utility of 3-methoxytyramine measurements. *Pharmacol. Rev.* **40**, 163–187.

Xu Y., Ola M. S., Berkich D. A. *et al.* (2007) Energy sources for glutamate neurotransmission in the retina: absence of the aspartate/glutamate carrier produces reliance on glycolysis in glia. *J. Neurochem.* **101**, 120–131.

Yin F., Sancheti H. and Cadenas E. (2012) Silencing of nicotinamide nucleotide transhydrogenase impairs cellular redox homeostasis and energy metabolism in PC12 cells. *Biochim. Biophys. Acta* **1817**, 401–409.

Zeevalk G. D., Manzino L., Hoppe J. and Sonsalla P. (1997) In vivo vulnerability of dopamine neurons to inhibition of energy metabolism. *Eur. J. Pharmacol.* **320**, 111–119.

Zoccarato F., Toscano P. and Alexandre A. (2005) Dopamine-derived dopaminochrome promotes H_2O_2 release at mitochondrial complex I. *J. Biol. Chem.* **280**, 15587–15594.

Zweifel L. S., Fadok J. P., Argilli E. *et al.* (2011) Activation of dopamine neurons is critical for aversive conditioning and prevention of generalized anxiety. *Nat. Neurosci.* **14**, 620–626.

Clinical Neurology and Neurosurgery xxx (2013) xxx–xxx

Contents lists available at SciVerse ScienceDirect

Clinical Neurology and Neurosurgery

journal homepage: www.elsevier.com/locate/clineuro

Case report

A 73-year-old patient with adult-onset type II citrullinemia successfully treated by sodium pyruvate and arginine

Masahide Yazaki[a,*], Michiaki Kinoshita[a], Shinji Ogawa[b], Satoshi Fujimi[b], Akira Matsushima[a], Akiyo Hineno[a], Ko-ichi Tazawa[a], Kazuhiro Fukushima[a], Ryo Kimura[c], Makoto Yanagida[c], Hidenori Matsunaga[c], Takeyori Saheki[d], Shu-ichi Ikeda[a]

[a] Department of Medicine (Neurology and Rheumatology), Shinshu University School of Medicine, Matsumoto 390-8621, Japan
[b] Department of Emergency and Critical Care, Osaka General Medical Center, Osaka, Japan
[c] Department of Psychiatry, Osaka General Medical Center, Osaka, Japan
[d] Institute of Resource Development and Analysis, Kumamoto University, Kumamoto, Japan

ARTICLE INFO

Article history:
Received 28 February 2012
Received in revised form
17 December 2012
Accepted 22 December 2012
Available online xxx

Keywords:
Citrin deficiency
CTLN2
Aged patients
Hepatic encephalopathy
Sodium pyruvate

1. Introduction

Citrin deficiency, caused by a mutation of the *SLC25A13* gene, is an autosomal recessive disorder that leads to neonatal intrahepatic cholestasis caused by citrin deficiency (NICCD) and adult-onset type II citrullinemia (CTLN2) [1]. The function of citrin is important in translocating cytosolic NADH reducing equivalents into the mitochondria as part of the malate-aspartate shuttle [2]. In addition, citrin plays an important role in supplying aspartate to argininosuccinate synthetase (ASS) in the cytosol to generate argininosuccinate in the urea cycle [2]. Thus, a deficiency of citrin results in dysfunction of the urea cycle and hyperammonemia [1]. Patients with CTLN2 present with sudden onset of various encephalopathic manifestations due to hyperammonemia [2]. One of the distinct features of citrin deficiency is that the majority of patients have a peculiar fondness for protein- and fat-rich foods, such as beans and peanuts, and an aversion to carbohydrate-rich foods, such as rice, sweets, and alcohol [2]. It is assumed that their unique food preference may be directly related to the pathophysiology associated with loss of citrin function, as a mitochondrial aspartate (Asp)-glutamate (Glu) carrier (AGC) in the malate-aspartate shuttle, resulting in an increase of cytosolic NADH/NAD ratio [2]. The mean age of onset of CTLN2 is in the fourth decade [2] but its range was described to be very wide from 11 to 79 years [3]. However, as there have been no detailed case reports regarding elderly CTLN2 patients [3], the clinical features and optimal therapeutic strategy in elderly CTLN2 patients remain unclear. Here, we report a rare case of CTLN2 with onset of the disease at 73 years old. The patient was treated successfully with sodium pyruvate [4] in combination with arginine granule [5] and dietary adjustments without undergoing liver transplantation.

2. Case report

The patient was a Japanese woman admitted to a local hospital because of sudden onset of consciousness disturbance in August 2010 at aged 73. Her consciousness improved within a few days but the etiology of disturbed consciousness remained unclear. In September, she became drowsy and highly confused. She was thought to have psychiatric disorders and was transferred to Osaka General Medical Center in late September. In October, however, her condition rapidly worsened and she became comatose.

* Corresponding author. Tel.: +81 263 37 2673.
E-mail address: mayazaki@shinshu-u.ac.jp (M. Yazaki).

0303-8467/$ – see front matter
http://dx.doi.org/10.1016/j.clineuro.2012.12.027